THE JOURNAL OF BIOLOGICAL CHEMISTRY VOL. 283, NO. 35, pp. 24234–24244, August 29, 2008

Interaction of Scaffolding Adaptor Protein Gab1 with Tyrosine Phosphatase SHP2 Negatively Regulates IGF-I-dependent Myogenic Differentiation via the ERK1/2 Signaling Pathway*[S]

Received for publication, May 21, 2008, and in revised form, June 18, 2008 Published, JBC Papers in Press, June 23, 2008, DOI 10.1074/jbc.M803907200

Tatsuya Koyama[‡§1], Yoshikazu Nakaoka[‡¶1,2], Yasushi Fujio[‖], Hisao Hirota[¶†], Keigo Nishida[**], Shoko Sugiyama[¶], Kitaro Okamoto[¶], Keiko Yamauchi-Takihara[¶], Michihiro Yoshimura[§], Seibu Mochizuki[§], Masatsugu Hori[¶], Toshio Hirano[‡‡], and Naoki Mochizuki[‡]**

From the [‡]Department of Structural Analysis, National Cardiovascular Center Research Institute, 5-7-1, Fujishirodai, Suita, Osaka, 565-8565, the [¶]Department of Cardiovascular Medicine, Osaka University Graduate School of Medicine, 2-2, Yamadaoka, Suita, Osaka, 565-0871, the [‖]Department of Clinical Pharmacology and Pharmacogenomics, Osaka University Graduate School of Pharmaceutical Sciences, 1-6, Yamadaoka, Suita, Osaka, 565-0871, the [**]Laboratory for Cytokine Signaling, RIKEN Research Center for Allergy and Immunology, 1-7-22, Suehiro-cho, Tsurumi-ku, Yokohama City, Kanagawa, 230-0045, the [§]Division of Cardiology, Department of Internal Medicine, The Jikei University School of Medicine, 3-25-8, Nishi-Shinbashi, Minato-ku, Tokyo, 105-8461, and the [‡‡]Laboratory of Developmental Immunology, Osaka University Graduate School of Frontier Biosciences and Graduate School of Medicine, 2-2, Yamadaoka, Suita, Osaka, 565-0871, Japan

Grb2-associated binder 1 (Gab1) coordinates various receptor tyrosine kinase signaling pathways. Although skeletal muscle differentiation is regulated by some growth factors, it remains elusive whether Gab1 coordinates myogenic signals. Here, we examined the molecular mechanism of insulin-like growth factor-I (IGF-I)-mediated myogenic differentiation, focusing on Gab1 and its downstream signaling. Gab1 underwent tyrosine phosphorylation and subsequent complex formation with protein-tyrosine phosphatase SHP2 upon IGF-I stimulation in C2C12 myoblasts. On the other hand, Gab1 constitutively associated with phosphatidylinositol 3-kinase regulatory subunit p85. To delineate the role of Gab1 in IGF-I-dependent signaling, we examined the effect of adenovirus-mediated forced expression of wild-type Gab1 ($Gab1^{WT}$), mutated Gab1 that is unable to bind SHP2 ($Gab1^{\Delta SHP2}$), or mutated Gab1 that is unable to bind p85 ($Gab1^{\Delta p85}$), on the differentiation of C2C12 myoblasts. IGF-I-induced myogenic differentiation was enhanced in myoblasts overexpressing $Gab1^{\Delta SHP2}$, but inhibited in those overexpressing either $Gab1^{WT}$ or $Gab1^{\Delta p85}$. Conversely, IGF-I-induced extracellular signal-regulated kinase 1/2 (ERK1/2) activation was significantly repressed in myoblasts overexpressing $Gab1^{\Delta SHP2}$ but enhanced in those overexpressing either $Gab1^{WT}$ or $Gab1^{\Delta p85}$. Furthermore, small interference RNA-mediated Gab1 knockdown enhanced myogenic differentiation. Overexpression of catalytic-inactive SHP2 modulated IGF-I-induced myogenic differentiation and ERK1/2 activation similarly to that of $Gab1^{\Delta SHP2}$, suggesting that Gab1-SHP2 complex inhibits IGF-I-dependent myogenesis through ERK1/2. Consistently, the blockade of ERK1/2 pathway reversed the inhibitory effect of $Gab1^{WT}$ overexpression on myogenic differentiation, and constitutive activation of the ERK1/2 pathway suppressed the enhanced myogenic differentiation by overexpression of $Gab1^{\Delta SHP2}$. Collectively, these data suggest that the Gab1-SHP2-ERK1/2 signaling pathway comprises an inhibitory axis for IGF-I-dependent myogenic differentiation.

Skeletal muscle differentiation is a multistep process in which multipotent mesodermal cells give rise to myoblasts that subsequently withdraw from the cell cycle and differentiate into multinucleated myotubes. Most skeletal muscle cell lines from rodents proliferate in high serum conditions containing various mitogens, and post-confluent cells spontaneously differentiate after several days in low serum conditions (1, 2). Among various growth factors, the insulin-like growth factors (IGFs),[3] includ-

* This work was supported by grants from the Ministry of Education, Science, Sports and Culture of Japan (to Y. N., K. Y.-T., and N. M.); the Ministry of Health, Labour, and Welfare of Japan (to N. M.); the Program for the Promotion of Fundamental Studies in Health Sciences of the National Institute of Biomedical Innovation (to N. M.); the Takeda Medical Research Foundation (to N. M.); The Uehara Memorial Foundation (to Y. N.); the Japan Heart Foundation Young Investigator's Research Grant (to Y. N.); the Suzuken Memorial Foundation (to Y. N.); the Astellas Foundation for Research on Metabolic Disorders (to Y. N.); the Senri Life Science Foundation (to Y. N.); and the Miyata Cardiology Research Promotion Funds (to Y. N.). The costs of publication of this article were defrayed in part by the payment of page charges. This article must therefore be hereby marked "*advertisement*" in accordance with 18 U.S.C. Section 1734 solely to indicate this fact.

[S] The on-line version of this article (available at http://www.jbc.org) contains supplemental text, references, and Figs. S1 and S2.

† Deceased on December 27, 2005.

[1] Both authors contributed equally to this work.

[2] To whom correspondence should be addressed: Dept. of Cardiovascular Medicine, Osaka University Graduate School of Medicine, Suita, Osaka 565-0871, Japan. Tel.: 81-6-6879-3835; Fax: 81-6-6879-3839; E-mail: ynakaoka@imed3.med.osaka-u.ac.jp.

[3] The abbreviations used are: IGF, insulin-like growth factor; Gab1, Grb2-associated binder 1; Gab2, Grb2-associated binder 2; WT, wild-type; PI3K, phosphatidylinositol 3-kinase; MAPK, mitogen-activated protein kinase; MEK1/2, MAPK/extracellular signal-regulated kinase kinase 1/2; ERK1/2, extracellular signal-regulated kinase 1/2; SH2, Src homology 2; SHP2, SH2-containing protein-tyrosine phosphatase 2; EGF, epidermal growth factor; VEGF, vascular endothelial growth factor; IRS-1, insulin receptor substrate-1; MHC, myosin heavy chain; DMEM, Dulbecco's modified Eagle's medium; FBS, fetal bovine serum; β-gal, β-galactosidase; HS, horse serum; FGF2, fibroblast growth factor 2; IP, immunoprecipitation; ANOVA, analysis of variance; siRNA, small interference RNA; RNAi, RNA interference.

ing IGF-I and IGF-II, have been reported to be quite unique in that they stimulate both proliferation and differentiation of muscle cells in culture (3, 4). IGF-I receptor belongs to the receptor tyrosine kinase family and utilizes two major cytoplasmic signaling pathways, namely the phosphatidylinositol 3-kinase (PI3K) cascade and mitogen-activated protein kinase (MAPK) cascade, which consists of Raf-MAPK/extracellular signal-regulated kinase (ERK)-kinase1/2 (MEK1/2)-ERK1/2 (5). PI3K is one of the primary signaling molecules promoting skeletal muscle differentiation, as demonstrated by pharmacological and genetic methods (3, 6, 7). On the other hand, activation of Raf-MEK1/2-ERK1/2 MAPK cascade has been reported to have inhibitory effects on the myogenic differentiation induced by insulin or IGFs (3, 8–10).

Grb2-associated binder 1 (Gab1) belongs to the scaffolding adaptor protein family. Gab1 has an N-terminal pleckstrin homology domain, as well as multiple tyrosine-based motifs and proline-rich sequences, which are potential binding sites for various Src homology 2 (SH2) domains and Src homology 3 domains, respectively. Gab1 undergoes tyrosine phosphorylation upon stimulation with various growth factors, cytokines, G protein-coupled receptor agonists, and various immuno-antigens (11,12). Tyrosine-phosphorylated Gab1 provides docking sites for multiple SH2 domain-containing signaling molecules, such as SH2-containing protein-tyrosine phosphatase SHP2, PI3K regulatory subunit p85, phospholipase C-γ, Crk, and Ras GTPase-activating protein (11–17). Among these binding partners, SHP2, a ubiquitously expressed protein-tyrosine phosphatase, has crucial roles for receptor tyrosine kinase-dependent activation of ERK1/2 in association with Gab1 (18, 19). The functional significance of Gab1-SHP2 interaction has been extensively studied using the Gab1 mutant that is unable to bind SHP2. This Gab1 mutant is defective in delivering signals for hepatocyte growth factor-c-Met-dependent morphogenesis, epidermal growth factor (EGF)-dependent epidermal proliferation, and leukemia inhibitory factor-gp130-dependent cardiomyocyte hypertrophy (20–23). These findings underscore the importance of Gab1-SHP2 interaction and strongly suggest that the primary role of Gab1 might be to recruit SHP2 (24). On the other hand, it has been reported that Gab1 also regulates the PI3K-AKT signaling pathway through association with p85 downstream of various growth factors (25–29). Gab1 has been reported to be required for both EGF-dependent activation of PI3K-AKT signaling pathway and migration of keratinocytes (28–30). In addition, Gab1 plays a key role for vascular endothelial growth factor-dependent activation of the PI3K signaling pathway and is required for endothelial cell migration and capillary formation (25, 27).

Gab1knockout (Gab1KO) mice died *in utero* and displayed developmental defects in the heart, placenta, liver, skin, and skeletal muscle (31, 32). Furthermore, Gab1KO mice displayed reduced and delayed migration of muscle progenitor cells into the limbs and diaphragm, resulting in the immature formation of limb muscles. These data suggest that Gab1 might have a key role in skeletal muscle development (32). We created cardiomyocyte-specific Gab1/Gab2 double knock-out mice and revealed that Gab1 and Gab2 play redundant, but essential roles in postnatal maintenance of cardiac function via the neuregulin-1/ErbB signaling pathway (33). In addition, liver-specific Gab1 knock-out mice displayed enhanced hepatic insulin sensitivity with reduced glycemia and improved glucose tolerance as a result of insufficient insulin-elicited activation of ERK1/2 (34). However, it remains elusive whether Gab1 has a specific role in skeletal muscle differentiation. In this study, we demonstrate for the first time that Gab1-SHP2 interaction exerts an inhibitory effect on IGF-I-induced myogenic differentiation via activation of the ERK1/2 signaling pathway.

EXPERIMENTAL PROCEDURES

Reagents and Antibodies—Anti-phospho-p44/42 ERK1/2 (Thr-202/Tyr-204), anti-phospho-AKT (Thr-308), anti-ERK1/2, and anti-AKT antibodies were purchased from Cell Signaling Technology. Anti-Gab1 and anti-Gab2 sera for immunoprecipitation were described previously (15, 16, 22). The antibodies against the following molecules used for immunoblotting, Gab1, Gab2, insulin receptor substrate-1 (IRS-1), and p85 PI3K were from Millipore; PY99, SHP2, MEK1, and myogenin were from Santa Cruz Biotechnology. Anti-myosin heavy chain (MHC) monoclonal antibody (MF20) was purchased from the Developmental Hybridoma Bank (Dr. D. A. Fischman, University of Iowa, Iowa City, IA). Hoechst 33342 nuclear dye was from Sigma. Horseradish peroxidase-conjugated anti-mouse and anti-rabbit antibodies were from GE Health Science. U0126 was from Promega (Madison, WI). Serum and cell culture reagents were from Invitrogen. Human recombinant IGF-I was kindly provided by Astellas Pharmaceuticals.

Adenovirus Vector Construction—The generation of adenovirus vectors expressing human Gab1^{WT} and Gab1$^{\Delta SHP2}$ (mutated on the two tyrosine residues responsible for binding with SHP2) were described previously (22). In this study, we constructed the adenovirus vectors expressing Gab1$^{\Delta p85}$, which can't bind with p85 due to the substitution of tyrosine residues 447, 472, and 589 of human Gab1, corresponding to the *YXXM* motifs, to phenylalanines by PCR-based mutagenesis described previously (35). Substitution of these tyrosine residues by phenylalanine renders the molecule incapable of binding with p85. We also constructed adenovirus vectors expressing wild-type SHP2 (SHP2^{WT}) and phosphatase-inactive SHP2 (SHP2$^{C/S}$) using the plasmid vectors described previously (15). For adenovirus production, the sequence encoding Gab1$^{\Delta p85}$, SHP2^{WT}, or SHP2$^{C/S}$ was subcloned into the shuttle plasmid pACCMVpLpA. Recombinant adenoviruses were then obtained according to the homologous recombination system described elsewhere (36). The adenovirus vectors expressing constitutive-active MEK1 and dominant-negative MEK1 were kindly provided by Dr. S. Kawashima (Kobe University) and described previously (37). The construction of adenovirus vector expressing human Gab2$^{\Delta SHP2}$, which can't bind with SHP2, is described in the supplemental data.

Cell Culture, Stimulation, and Adenoviral Infection—C2C12 murine myoblast cells were maintained as subconfluent monolayers in Dulbecco's modified Eagle's medium (DMEM) containing 4.5 g/liter glucose, 0.58 g/liter L-glutamine, 100 units/ml penicillin, and 100 μg/ml streptomycin supplemented with

20% fetal bovine serum (FBS). Before stimulation, cells were serum-starved overnight. Stimulations were performed using 80 ng/ml IGF-I for 10 min, unless otherwise indicated. For adenoviral infection of C2C12 myoblasts, subconfluent cells were cultured in DMEM with 20% FBS at a multiplicity of infection of 50 for 24 h. In the dual infection of adenovirus vectors, C2C12 cells were cultured in DMEM with 20% FBS with each virus at a multiplicity of infection of 30. Then, the myoblasts were serum-starved overnight and stimulated with or without IGF-I for the experiments examining ERK1/2 and AKT phosphorylation. Infection efficiency, determined by *lacZ* gene expression in cultured myoblasts, is consistently >90% with this method. Adenovirus vector expressing β-galactosidase (β-gal) was used as a control. For the induction of myogenic differentiation, cultured medium was switched from DMEM containing 20% FBS to DMEM containing 2% horse serum (HS) or 80 ng/ml IGF-I, when cell density reached confluency. The differentiation medium containing 2% HS was exchanged every other day, and that containing IGF-I was exchanged every day.

Cell Lysis, Immunoprecipitations, and Immunoblotting—Cells were scraped off in lysis buffer containing 20 mM Tris (pH 7.4), 150 mM NaCl, 3 mM EDTA, 1% Nonidet P-40, 2 mM sodium orthovanadate, and protease inhibitor mixture Complete (Roche Applied Science). Cell lysates were collected form confluent 6-cm dishes and precleared by 15,000 × *g* centrifugation for 15 min. For immunoprecipitation, the cleared lysates of 500 μl containing 1 mg of protein, were rotationally incubated with 1 μl of anti-Gab1 antiserum, or 1.2 μg of SHP2 antibody, or 5 μl of p85 antibody, or 10 μl of IRS-1 antibody and with 20 μl of protein A-Sepharose (GE Healthcare) overnight at 4 °C. The antigen-antibody complexes were collected by centrifugation, washed three times with lysis buffer without protease inhibitor mixture, and boiled in standard electrophoresis sample buffer. All the proteins immunoprecipitated were then resolved by SDS-PAGE and subjected to immunoblotting using a standard procedure. Blots were developed using ECL system (GE Healthcare). For direct immunoblotting analyses, the crude cell lysates were collected from 3.5-cm dishes and subjected to 15,000 × *g* centrifugation. The precleared lysates containing 30 μg of protein were loaded in each lane for immunoblotting.

Immunocytochemistry—Cells cultured on 3.5-cm collagen type I-coated plastic dishes (Iwaki Asahi Glass Co.) were fixed with 2% formaldehyde in phosphate-buffered saline and permeabilized with 0.1% Triton X-100 for 10 min. Cells were blocked with phosphate-buffered saline containing 1% bovine serum albumin for 1 h and incubated with anti-MHC antibody (MF20), followed by incubation with Alexa 488-labeled goat anti-mouse secondary antibody (Molecular Probes). Cells were post-stained with Hoechst 33342 nuclear dye and viewed by fluorescence microscopy.

siRNA-mediated Protein Knockdown—Stealth Select small interfering RNAs (siRNAs) targeted to murine Gab1 (#1, MSS204497; #2, MSS204499) and siRNA duplex with irrelevant sequences (Stealth™ RNAi negative control) as a control were purchased from Invitrogen. Stealth siRNAs targeted to murine SHP2 were purchased from Invitrogen. and the detailed sequences are described in the supplemental data. C2C12 myoblasts were transfected with 10 nM siRNA duplexes using Lipofectamine™ RNAiMAX reagent according to the manufacturer's instructions for reverse transfection. Briefly, C2C12 myoblasts (1.5×10^5 cells per each dish) were diluted in 860 μl of DMEM containing 20% FBS and plated on 3.5-cm collagen type I-coated plastic dishes. To each dish, 140 μl of RNAi duplex-Lipofectamine™ RNAiMAX complex diluted in Opti-MEM I medium was added. After incubation for 72 h, the cells were used for the experiments.

Statistics—All data are expressed as mean ± S.D. Differences among multiple groups were compared by one-way ANOVA followed by a post hoc comparison tested with Scheffe's method. Values of $p < 0.05$ were considered significant.

RESULTS

Gab1 Undergoes Tyrosine Phosphorylation and Subsequently Associates with SHP2 upon IGF-I Stimulation in C2C12 Myoblasts—We examined the effect of IGF-I on tyrosine-phosphorylation of Gab1 and its association with SH2 domain-containing signaling molecules in C2C12 myoblasts. IGF-I indeed induced tyrosine phosphorylation of Gab1 and subsequent association of Gab1 with SHP2 in C2C12 myoblasts (Fig. 1*A*, *left panel*). Furthermore, SHP2 was also tyrosine-phosphorylated and associated with Gab1 after stimulation with IGF-I (Fig. 1*A*, *right panel*). On the other hand, Gab1 constitutively associated with p85 both before and after IGF-I stimulation (Fig. 1*A*, *left panel*). In the IGF-I-dependent signaling pathway, IRS-1 has been reported to be a major binding partner of p85 and essential for IGF-I-dependent PI3K-AKT signaling in skeletal muscle cells (38). Consistently, IRS-1 underwent strong tyrosine phosphorylation after stimulation with IGF-I in C2C12 myoblasts. In clear contrast to Gab1, IRS-1 associated with p85 in a manner dependent on IGF-I stimulation (Fig. 1*B*). In addition, we could not detect the complex formation of IRS-1 with SHP2 either before or after stimulation with IGF-I (Fig. 1*B*). These results demonstrate that IGF-I induces tyrosine phosphorylation of Gab1, leading to complex formation of Gab1 with SHP2 in C2C12 myoblasts.

IGF-I-induced Tyrosine Phosphorylation of Gab1 and Association of Gab1 with SH2 Domain-containing Molecules in the C2C12 Myoblasts Infected with Adenovirus Vectors—IGFs have been reported to stimulate both proliferation and differentiation of cultured skeletal muscle cells (3, 4). The effect of IGF-I on the proliferation of myoblasts has been reported to be attributed mainly to ERK1/2 pathway (3). In the present study, we tried to reveal the role of Gab1 in IGF-I-dependent differentiation from myoblasts into myotubes. To discern the role of Gab1-SHP2 interaction from that of Gab1-p85 interaction in IGF-I-dependent differentiation, we used recombinant adenovirus vectors carrying β-gal (control), $Gab1^{WT}$, or $Gab1^{\Delta SHP2}$ as described previously (22) and created an adenovirus vector overexpressing $Gab1^{\Delta p85}$. We examined tyrosine phosphorylation of Gab1 upon stimulation with IGF-I in myoblasts overexpressing β-gal, $Gab1^{WT}$, $Gab1^{\Delta SHP2}$, or $Gab1^{\Delta p85}$. As shown in Fig. 2*A*, tyrosine phosphorylation of Gab1 and the amount of co-immunoprecipitated SHP2 with Gab1 were increased after stimulation with IGF-I in control myoblasts expressing β-gal. On the other hand, tyrosine phosphorylation of Gab1 in the

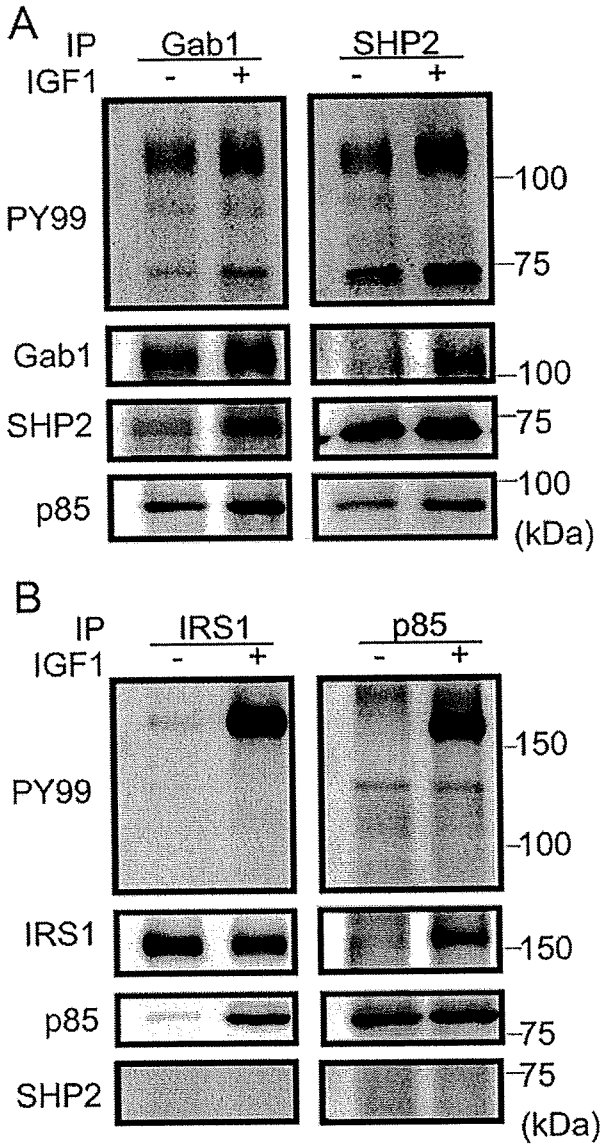

FIGURE 1. **IGF-I induces tyrosine phosphorylation of Gab1 and complex formation of Gab1 with SHP2 in C2C12 myoblasts.** Serum-starved C2C12 myoblast cells were stimulated with 80 ng/ml IGF-I for 10 min, and cell lysates of 500 μl harvested from 6 cm dishes were subjected to immunoprecipitation analysis with anti-Gab1 serum (*A, left panel*), anti-SHP2 antibody (*A, right panel*), anti-IRS-1 antibody (*B, left panel*), or anti-p85 antibody (*B, right panel*). Immunoprecipitates were subjected to SDS-PAGE followed by immunoblot analysis with anti-phosphotyrosine antibody (PY99). The same membrane was reprobed with the antibodies indicated at the *left* (anti-Gab1, anti-SHP2, and anti-p85 antibodies). *A*, both Gab1 and SHP2 were tyrosine-phosphorylated and co-immunoprecipitated with each other in an IGF-I-dependent manner. On the other hand, the association of Gab1 with p85 did not change either before or after IGF-I treatment. *B*, upon stimulation with IGF-I, IRS-1 became strongly tyrosine-phosphorylated and co-immunoprecipitated with p85. However, co-immunoprecipitation of IRS-1 with SHP2 was not detected. Experiments were repeated three times with similar results.

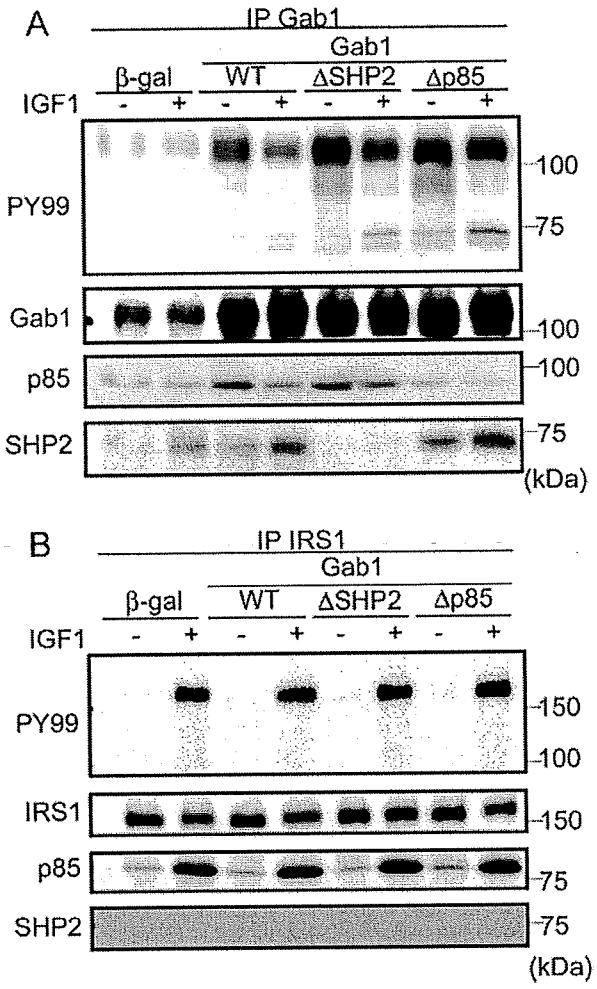

FIGURE 2. **Overexpression of Gab1$^{\Delta SHP2}$ or Gab1$^{\Delta p85}$ specifically perturbs the IGF-I-dependent molecular association of Gab1 with SHP2 or p85, respectively.** C2C12 myoblasts were infected with adenovirus vectors expressing β-gal, Gab1^{WT}, Gab1$^{\Delta SHP2}$, or Gab1$^{\Delta p85}$. Serum-starved C2C12 cells were stimulated with vehicle (−) or IGF-I for 10 min, and cell lysates of 500 μl were collected from 6-cm dishes. Cell lysates were subjected to immunoprecipitation with anti-Gab1 serum (*A*) or with anti-IRS-1 antibody (*B*), followed by immunoblotting with anti-phosphotyrosine antibody (PY99). *A*, blots were reprobed with anti-Gab1, anti-p85, and anti-SHP2 antibodies. *B*, blots were reprobed with anti-IRS-1, anti-p85, and anti-SHP2 antibodies. Experiments were repeated three times with similar results.

myoblasts overexpressing Gab1^{WT}, Gab1$^{\Delta SHP2}$, or Gab1$^{\Delta p85}$ increased much more at baseline compared with in those overexpressing β-gal. In these cells, tyrosine phosphorylation of Gab1 decreased after stimulation with IGF-I. The IGF-I-induced association of Gab1 with SHP2 increased in the C2C12 myoblasts overexpressing Gab1^{WT}, or Gab1$^{\Delta p85}$ compared with those overexpressing β-gal, but was almost abrogated in those overexpressing Gab1$^{\Delta SHP2}$ (Fig. 2*A*). The co-immunoprecipitation of Gab1 with p85 was increased in cells expressing Gab1^{WT} or Gab1$^{\Delta SHP2}$ compared with those expressing β-gal, but was almost abrogated in those expressing Gab1$^{\Delta p85}$ at the baseline. The association of Gab1 with p85 decreased in response to IGF-I in the cells overexpressing Gab1^{WT} or Gab1$^{\Delta SHP2}$ (Fig. 2*A*). We observed much more dissociation of p85 from Gab1 in myoblasts overexpressing Gab1^{WT} compared with those overexpressing Gab1$^{\Delta SHP2}$, which might be attributed to the increased activation of SHP2. Presumably, SHP2 dephosphorylates the tyrosine residues for p85 binding site of Gab1 consistent with the previous report on EGF-dependent signaling (39). These data demonstrate that overexpression of

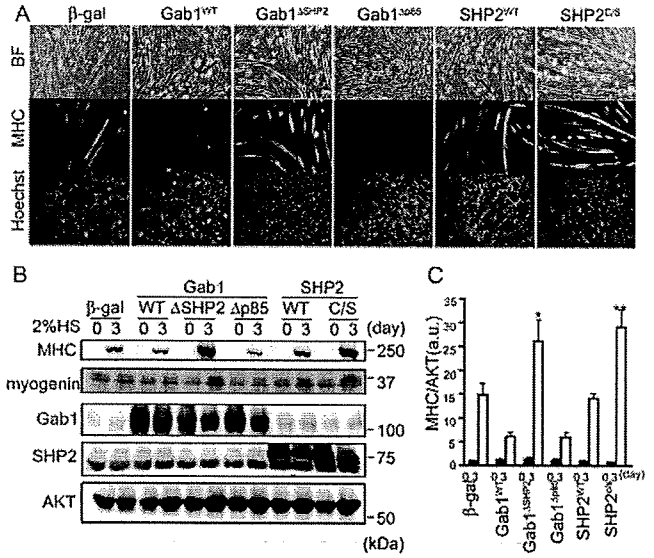

FIGURE 3. **Myogenic differentiation in a low serum condition is negatively regulated by Gab1-SHP2 complex through activating phosphatase activity of SHP2 in C2C12 myoblasts.** *A*, immunocytochemical analysis of C2C12 myoblasts using anti-MHC antibody. C2C12 myoblasts were infected with adenovirus vectors expressing β-galactosidase (β-gal), $Gab1^{WT}$, $Gab1^{\Delta SHP2}$, $Gab1^{p85}$, $SHP2^{WT}$, or $SHP2^{C/S}$ and induced into myogenic differentiation by switching the growth medium containing 20% fetal bovine serum to the differentiation medium containing 2% horse serum. On the third day after induction, cells were immunostained with anti-MHC antibody and post-stained with nuclear dye Hoechst 33342. *BF*, bright field image. Experiments were repeated three times with similar results. *B*, Western blot analysis of myoblasts infected with indicated adenovirus vectors before and after low serum-induced myogenic induction for 3 days. Cell lysates were subjected to Western blot analysis using anti-MHC and anti-myogenin antibodies. The membrane was stripped and reprobed with anti-Gab1 or anti-SHP2 antibodies for confirmation of adenoviral overexpression of Gab1 or SHP2. AKT expression was also examined for loading control. *C*, the relative expression level of MHC was quantified by normalizing the expression of MHC by that of AKT. Values are expressed as means ± S.D. of three independent experiments (*, $p < 0.05$ or **, $p < 0.01$ compared with control cells expressing β-gal on the same day after myogenic induction, by one-way ANOVA). *a.u.*, arbitrary unit(s).

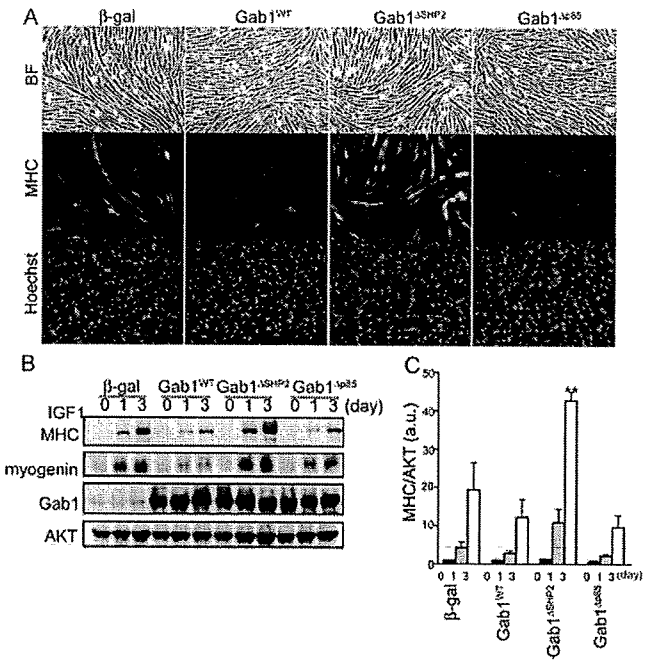

FIGURE 4. **IGF-I-induced myogenic differentiation is negatively regulated by interaction of Gab1 with SHP2 in C2C12 myoblasts.** *A*, immunocytochemical analysis of C2C12 myoblasts overexpressing various Gab1 proteins. C2C12 myoblasts infected with adenovirus vectors overexpressing β-gal, $Gab1^{WT}$, $Gab1^{\Delta SHP2}$, or $Gab1^{\Delta p85}$ (as indicated at the top), were cultured in differentiation medium containing IGF-I. On the third day after exposure to the differentiation medium containing IGF-I, cells were immunostained with anti-MHC antibody and post-stained with Hoechst 33342 nuclear dye. Experiments were repeated three times with similar results. *B*, cell lysates were collected from C2C12 cells overexpressing β-gal, $Gab1^{WT}$, $Gab1^{\Delta SHP2}$, or $Gab1^{\Delta p85}$ at the indicated time after cultivation in the differentiation medium containing IGF-I. Cell lysates were subjected to Western blot analysis for analyzing the expression of MHC and myogenin. The membrane was reprobed with anti-Gab1 antibody for confirmation of adenoviral overexpression of Gab1. AKT was also examined as a loading control. *C*, the relative expression level of MHC was quantified by normalizing the expression of MHC by that of AKT. Values are shown as mean ± S.D. of three independent experiments (**, $p < 0.01$ compared with control cells expressing β-gal on the same day after myogenic induction, by one-way ANOVA). *a.u.*, arbitrary unit(s).

$Gab1^{\Delta SHP2}$ or $Gab1^{\Delta p85}$ sufficiently suppresses the association of Gab1 with SHP2 or p85, respectively.

On the other hand, tyrosine phosphorylation of IRS-1 and interaction between IRS-1 and p85 were comparable among the four groups of cells after stimulation with IGF-I (Fig. 2*B*). Thus, these findings indicate that overexpression of $Gab1^{\Delta SHP2}$ or $Gab1^{\Delta p85}$ specifically perturbs the IGF-I-dependent interaction of Gab1 with SHP2 or p85, respectively.

Myogenic Differentiation Induced by a Low Serum Condition Is Negatively Regulated by Gab1-SHP2 Complex through Activating SHP2 in C2C12 Myoblasts—C2C12 myoblasts undergo myogenic differentiation under a low-serum condition such as 2% HS (1, 2). Therefore, we examined the effects of overexpression of $Gab1^{WT}$, $Gab1^{\Delta SHP2}$, or $Gab1^{\Delta p85}$, on myogenic differentiation under low serum condition. After infection with adenovirus vectors for 24 h, confluent C2C12 myoblasts were cultured in the DMEM containing 2% HS. On the third day after induction of myogenic differentiation, cells were immunostained with anti-MHC antibody for evaluation of myogenic differentiation. The extent of myogenic differentiation was enhanced in myoblasts overexpressing $Gab1^{\Delta SHP2}$, but inhibited in myoblasts overexpressing either $Gab1^{WT}$ or $Gab1^{\Delta p85}$, compared with myoblasts infected with control adenovirus vector expressing β-gal (Fig. 3*A*). Western blot analysis also revealed that the expression of MHC was significantly increased by the overexpression of $Gab1^{\Delta SHP2}$, but seemed to be repressed by the overexpression either $Gab1^{WT}$ or $Gab1^{\Delta p85}$, compared with control (Fig. 3, *B* and *C*). These findings indicate that Gab1-SHP2 interaction exerts an inhibitory effect on myogenic differentiation induced by a low serum condition.

Gab1-SHP2 complex formation has been reported to result in an increase of phosphatase activity of SHP2 upon stimulation with EGF (20, 21, 24). To confirm the requirement of catalytic activity of SHP2 for inhibition of myogenesis, we created adenovirus vectors expressing wild-type SHP2 ($SHP2^{WT}$) and phosphatase-inactive SHP2 ($SHP2^{C/S}$). After infection with adenovirus vectors for 24 h, confluent C2C12 myoblasts were cultured in the DMEM containing 2% HS. The extent of myogenic differentiation determined by immunocytochemistry was enhanced in myoblasts overexpressing $SHP2^{C/S}$ compared with myoblasts overexpressing β-gal or $SHP2^{WT}$ (Fig. 3*A*). Consistently, Western blot analysis showed that overexpression of $SHP2^{C/S}$ in C2C12 cells induced significant increase of MHC

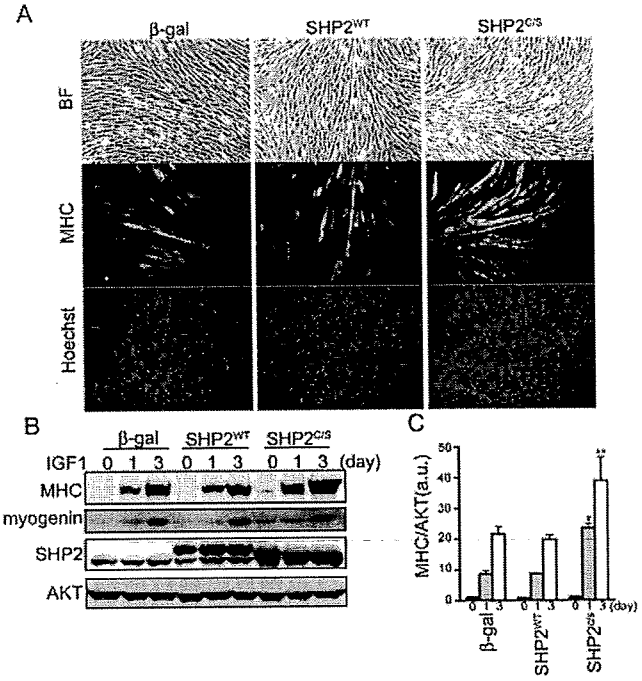

FIGURE 5. **SHP2 phosphatase activity is required for inhibition of myogenic differentiation.** *A*, C2C12 myoblasts overexpressing β-gal, $SHP2^{WT}$, or $SHP2^{C/S}$ were cultured in differentiation medium containing IGF-I. On the third day after exposure to the differentiation medium, cells were immunostained with anti-MHC antibody and post-stained with Hoechst 33342 nuclear dye. Myogenic differentiation was enhanced in myoblasts overexpressing $SHP2^{C/S}$ compared with myoblasts overexpressing β-gal and $SHP2^{WT}$. Experiments were repeated three times with similar results. *B*, cell lysates were collected from C2C12 cells overexpressing β-gal, $SHP2^{WT}$, or $SHP2^{C/S}$ at the indicated time after cultivation in the differentiation medium containing IGF-I. Cell lysates were subjected to Western blot analysis for analyzing the expression of MHC and myogenin. The membrane was reprobed with anti-SHP2 antibody for confirmation of adenoviral overexpression of SHP2. AKT was examined as a loading control. *C*, the relative expression level of MHC was quantified by normalizing the expression of MHC by that of AKT. Values are shown as means ± S.D. (*, $p < 0.05$ or **, $p < 0.01$ compared with control cells expressing β-gal on the same day after myogenic induction, by one-way ANOVA). *a.u.*, arbitrary unit(s).

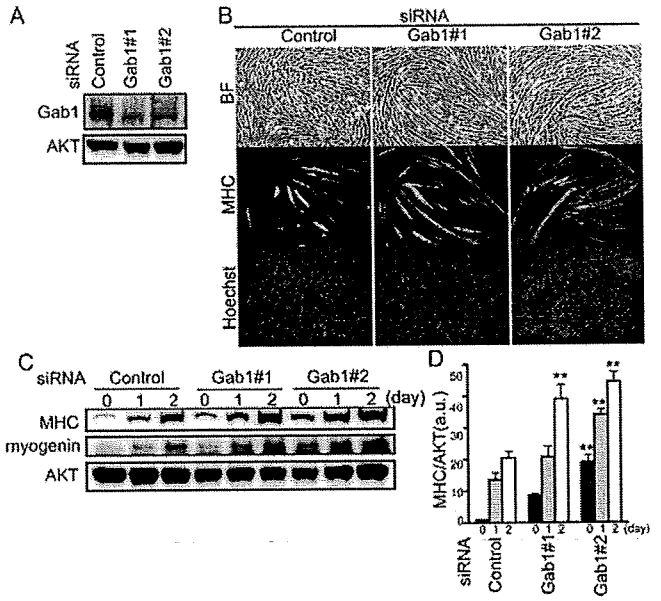

FIGURE 6. **siRNA-mediated Gab1 knockdown enhances myogenic differentiation.** *A*, C2C12 myoblasts were transfected with control siRNA (control) or with two independent siRNAs targeting different sequences of Gab1 (Gab1#1 and Gab1#2) for 72 h. Cell lysates were subjected to Western blot analysis. AKT was also checked as a loading control. *B*, C2C12 myoblasts were transfected with siRNAs as described in Fig. 6*A*. On the third day after transfection, the medium was changed from growth medium containing 20% FBS to differentiation medium containing 80 ng/ml IGF-I. Cells were cultured in the presence of IGF-I for 2 days. Cells were immunostained with anti-MHC antibody and post-stained with Hoechst 33342 nuclear dye. Experiments were repeated three times with similar results. *C*, cell lysates were collected at the indicated time after induction of myogenic differentiation and subjected to Western blot analysis. On the first and second day after myogenic induction, the expression level of MHC and myogenin were increased in cells transfected with Gab1 siRNAs (#1 or #2) compared with control. AKT was examined as a loading control. *D*, the relative expression level of MHC was quantified by normalizing the expression of MHC by that of AKT. Values are shown as means ± S.D. (**, $p < 0.01$ compared with control cells on the same day after myogenic induction, by one-way ANOVA). *a.u.*, arbitrary unit(s).

expression, compared with control (Fig. 3, *B* and *C*). Taken together, these findings suggest that Gab1 exerts an inhibitory effect on myogenic differentiation of C2C12 myoblasts under low serum condition through association with SHP2 and increase of SHP2 catalytic activity.

IGF-I-induced Myogenic Differentiation Is Negatively Regulated by Gab1-SHP2 Complex through Increasing Catalytic Activity of SHP2 in C2C12 Myoblasts—The IGF family, including IGF-I and -II, induces myogenic differentiation of myoblasts after myoblasts fully proliferate and become ready for differentiation (1–3). Therefore, we examined the effect of overexpression of various Gab1 proteins on the myogenic differentiation of C2C12 myoblasts cultured in IGF-I-containing differentiation medium. After infection with adenovirus vectors for 24 h, post-confluent C2C12 myoblasts were cultured in the DMEM containing 80 ng/ml IGF-I. On the third day after induction of myogenic differentiation, cells were immunostained with anti-MHC antibody. The extent of myogenic differentiation was enhanced in myoblasts overexpressing $Gab1^{\Delta SHP2}$ but inhibited in myoblasts overexpressing $Gab1^{WT}$ or $Gab1^{\Delta p85}$, compared with control (Fig. 4*A*). MHC expression was significantly increased in the myoblasts overexpressing $Gab1^{\Delta SHP2}$, although it seemed to be repressed in those overexpressing $Gab1^{WT}$ or $Gab1^{\Delta p85}$, compared with control (Fig. 4, *B* and *C*). Furthermore, the expression of myogenin was enhanced in myoblasts overexpressing $Gab1^{\Delta SHP2}$, but repressed in myoblasts overexpressing $Gab1^{WT}$ or $Gab1^{\Delta p85}$, compared with control (Fig. 4*B*). These data coincide with the results observed in the low serum condition, suggesting that Gab1-SHP2 complex has an inhibitory role in the IGF-I-induced myogenic differentiation.

Gab2, another Gab family protein, has been reported to complement the function of Gab1 in some signaling pathways such as EGF-dependent signaling (33, 40). To confirm the specific role of Gab1 in myogenic differentiation, we examined the effect of overexpression of $Gab2^{\Delta SHP2}$, the Gab2 mutant that cannot associate with SHP2 (41), on IGF-I-induced myogenic differentiation. The extent of myogenic differentiation was comparable between myoblasts overexpressing $Gab2^{\Delta SHP2}$ and those expressing β-gal (supplemental Fig. S1, *A* and *B*). We also confirmed that $Gab2^{\Delta SHP2}$ did not associate with SHP2 either before or after stimulation with IGF-I (supplemental Fig. S1*C*). These data suggested that IGF-I-induced myogenic differenti-

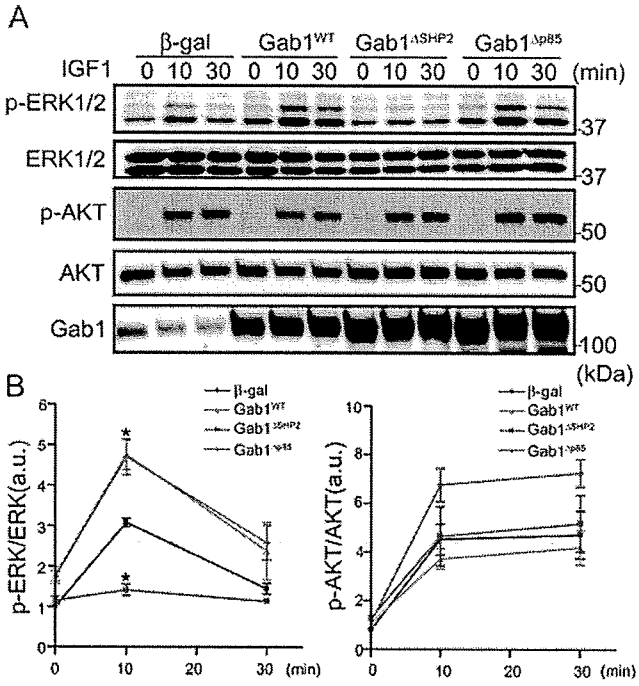

FIGURE 7. **IGF-I activates ERK1/2 via complex formation of Gab1 with SHP2 in C2C12 cells.** *A*, C2C12 cells infected with the indicated adenovirus vectors were serum-starved overnight and stimulated with IGF-I (80 ng/ml) for the indicated period. Cell lysates were collected at the indicated time and subjected to Western blot analysis using the antibodies indicated at the left. Expression level of Gab1 was almost comparable in the cells overexpressing $Gab1^{WT}$, $Gab1^{\Delta SHP2}$, or $Gab1^{\Delta p85}$. *B*, phosphorylation of ERK1/2 (*left*) and AKT (*right*) in *A* was quantified. Values are expressed as means ± S.D. of three independent experiments (*, $p < 0.05$, compared with control cells expressing β-gal at the same time after stimulation, by one-way ANOVA). *a.u.*, arbitrary unit(s).

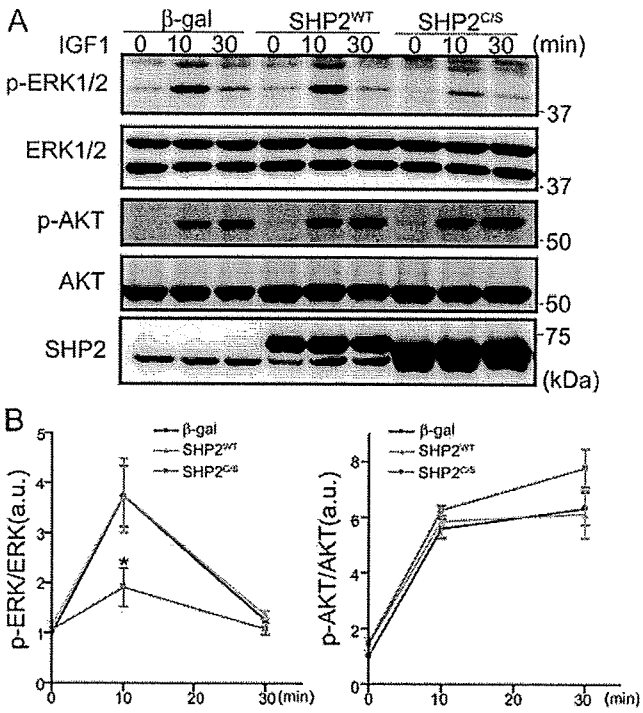

FIGURE 8. **IGF-I activates ERK1/2 via activation of SHP2 in C2C12 cells.** *A*, C2C12 cells infected with indicated adenovirus vectors were treated the same as in Fig. 7. Cell lysates were collected and subjected to Western blot analysis for analyzing ERK1/2 and AKT phosphorylation using the antibodies indicated at the left. Adenovirus-mediated overexpression of SHP2 was almost comparable in cells expressing $SHP2^{WT}$ or $SHP2^{C/S}$. *B*, phosphorylation of ERK1/2 (*left*) and AKT (*right*) in *A* was quantified. Values are shown as means ± S.D. from three independent experiments (*, $p < 0.05$ compared with control cells expressing β-gal at the same time after IGF-I stimulation, by one-way ANOVA). *a.u.*, arbitrary unit(s).

ation in C2C12 myoblasts might be regulated specifically by Gab1-SHP2 complex, but not by Gab2-SHP2 complex.

To confirm the requirement of SHP2 catalytic activity for the inhibitory effect of Gab1-SHP2 complex on myogenesis, C2C12 myoblasts were infected with adenovirus vectors expressing β-gal, $SHP2^{WT}$, or $SHP2^{C/S}$ and then treated with IGF-I-containing differentiation medium for the induction of myogenesis. Myogenic differentiation was enhanced in myoblasts overexpressing $SHP2^{C/S}$ compared with myoblasts overexpressing β-gal or $SHP2^{WT}$ (Fig. 5*A*). Western blot analysis also demonstrated that the MHC expression was significantly increased in the myoblasts overexpressing $SHP2^{C/S}$, but not in those overexpressing $SHP2^{WT}$, compared with control cells expressing β-gal (Fig. 5, *B* and *C*). Consistently, myogenin expression also seemed to be enhanced in those expressing $SHP2^{C/S}$, compared with myoblasts expressing β-gal or $SHP2^{WT}$ (Fig. 5*B*). These data indicate that Gab1-SHP2 complex has an inhibitory effect on IGF-I-elicited myogenic differentiation through activation of SHP2 in C2C12 myoblasts.

siRNA-mediated Knockdown of Gab1 Enhances Myogenic Differentiation in C2C12 Myoblasts—To examine the effect of Gab1 protein depletion in C2C12 myoblasts, we performed siRNA-mediated Gab1 knockdown. Gab1 protein expression was reduced by 80% in the myoblasts transfected with Gab1-targeted siRNAs compared with control cells (Fig. 6*A*). On the second day after induction of differentiation, cells were immunostained with anti-MHC antibody. The extent of myogenic differentiation was enhanced in myoblasts transfected with Gab1-targeted siRNAs compared with control (Fig. 6*B*). Consistently, Western blot analysis also revealed a significant increase of MHC expression in myoblasts transfected with Gab1-targeted siRNAs compared with control (Fig. 6, *C* and *D*). Furthermore, the expression of myogenin was increased in myoblasts transfected with Gab1-targeted siRNAs (Fig. 6*C*). These data coincide with the results obtained via overexpression experiments using adenovirus vectors and suggest that Gab1 has an inhibitory role in the IGF-I-induced myogenic differentiation.

Moreover, we performed siRNAs-mediated SHP2 knockdown in C2C12 myoblasts. SHP2 protein expression was reduced by 70% in the myoblasts transfected with SHP2-targeted siRNAs compared with control cells (supplemental Fig. S2*A*). On the contrary to the results obtained by Gab1-targeted siRNAs experiments, SHP2 knockdown inhibited proliferation of C2C12 myoblasts. Therefore, we could not evaluate the myogenic differentiation in C2C12 myoblasts transfected with SHP2-targeted siRNAs (supplemental Fig. S2*B*).

IGF-I-induced Activation of ERK1/2 Is Regulated by Gab1-SHP2 Complex through Activation of SHP2 in C2C12 Myoblasts—To elucidate a potential mechanism how Gab1 is involved in IGF-I-mediated myogenic differentiation of C2C12 myoblasts, we examined the effects of adenovirus-mediated overexpression of $Gab1^{WT}$, $Gab1^{\Delta SHP2}$, and $Gab1^{\Delta p85}$ on the

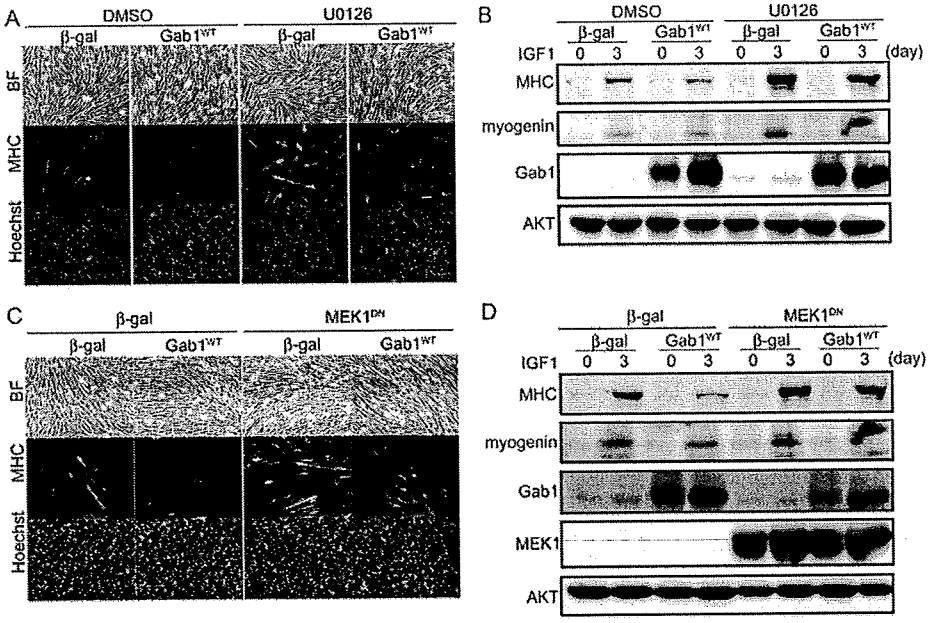

FIGURE 9. **ERK1/2 inhibition reverses the inhibitory effect of overexpression of Gab1^{WT} on IGF-I-induced myogenic differentiation.** *A*, C2C12 myoblasts were infected with adenovirus vectors overexpressing either β-gal or Gab1^{WT}. These cells were cultivated with or without a MEK1/2 inhibitor, U0126 (3 μM), under the differentiation medium containing 80 ng/ml IGF-I. On the third day after myogenic induction, the cells were immunostained with anti-MHC antibody and post-stained with Hoechst 33342 nuclear dye. Experiments were repeated three times with similar results. *B*, C2C12 cells overexpressing β-gal or Gab1^{WT} were cultured in the IGF-I-containing differentiation medium with or without U0126 (3 μM). Cell lysates were collected and subjected to Western blot analysis for analyzing the expression of MHC and myogenin. The membrane was reprobed with anti-Gab1 antibody for confirmation of adenoviral overexpression of Gab1. AKT was also checked as a loading control. *C*, C2C12 myoblasts were subjected to dual infection of adenovirus vectors expressing either β-gal or dominant-negative MEK1 (*MEK1^{DN}*) with Gab1^{WT}. On the third day after myogenic induction, the cells were immunostained with anti-MHC antibody and post-stained with Hoechst 33342 nuclear dye. Experiments were repeated three times with similar results. *D*, C2C12 myoblasts were subjected to dual infection of adenovirus vectors similarly to *B*. The cell lysates were collected and subjected to Western blot analysis for analyzing the expression of MHC and myogenin. The membrane was reprobed with anti-Gab1 and anti-MEK1 antibodies for confirmation of adenoviral overexpression of Gab1 and MEK1. AKT was also checked as a loading control. Experiments were repeated three times with similar results.

IGF-I-dependent signaling pathways downstream of Gab1. IGF-I induced activation of ERK1/2 and AKT in control myoblasts expressing β-gal. IGF-I-induced activation of ERK1/2 was significantly augmented in myoblasts overexpressing Gab1^{WT} or Gab1$^{\Delta p85}$ compared with control myoblasts expressing β-gal. On the other hand, activation of ERK1/2 was significantly reduced in myoblasts expressing Gab1$^{\Delta SHP2}$ (Fig. 7, *A* and *B*). On the other hand, activation of ERK1/2 was not changed in myoblasts expressing Gab2$^{\Delta SHP2}$ compared with control myoblasts expressing β-gal (supplemental Fig. S1*D*). These data indicate that Gab1 plays a critical role in IGF-I-induced ERK1/2 activation through interaction with SHP2 in C2C12 myoblasts.

IGF-I-induced AKT activation was almost comparable in myoblasts expressing β-gal, Gab1^{WT}, or Gab1$^{\Delta SHP2}$. On the contrary, activation of AKT seemed to be enhanced in cells overexpressing Gab1 $^{\Delta p85}$, compared with the other three groups (Fig. 7*B*). These data indicate that Gab1 might have a competitive role for sequestering p85 in the cytoplasm from other scaffolding adaptor proteins such as IRS-1.

To confirm the requirement of SHP2 activity for activation of ERK1/2 upon IGF-I stimulation, we examined the effects of adenovirus-mediated overexpression of SHP2^{WT} or SHP2$^{C/S}$ on ERK1/2 activation. IGF-I-induced activation of ERK1/2 was comparable in myoblasts overexpressing SHP2^{WT} and those expressing β-gal, but almost inhibited in cells overexpressing SHP2$^{C/S}$ compared with control (Fig. 8, *A* and *B*). On the other hand, activation of AKT was almost comparable among the three groups (Fig. 8, *A* and *B*). These findings indicate that SHP2 catalytic activity is indispensable for activation of ERK1/2 after stimulation with IGF-I in C2C12 myoblasts. Taken together, our findings indicate that IGF-I activates ERK1/2 via complex formation of Gab1 with SHP2 and activation of SHP2 in C2C12 myoblasts.

Gab1-SHP2-ERK1/2-signaling Pathway Is an Inhibitory Axis of IGF-I-dependent Myogenic Differentiation in C2C12 Myoblasts—It has been reported that ERK1/2 has an inhibitory role for myogenic differentiation of mesenchymal cells to date (3, 10). Therefore, we assumed that Gab1-SHP2 complex might have the inhibitory effects on myogenic differentiation via activation of ERK1/2. To confirm the inhibitory role of ERK1/2 downstream of Gab1-SHP2 complex, myoblasts overexpressing Gab1^{WT} were treated with or without a MEK1/2 inhibitor, U0126, before inducing myoblasts into myogenic differentiation in the presence of IGF-I. U0126 enhanced IGF-I-induced up-regulation of MHC and myogenin in control myoblasts expressing β-gal (Fig. 9, *A* and *B*). Furthermore, U0126 reversed the inhibitory effect of Gab1^{WT} overexpression on up-regulation of MHC and myogenin (Fig. 9, *A* and *B*). We also confirmed that adenovirus-mediated overexpression of dominant-negative MEK1 (MEK1^{DN}) reversed the inhibitory effect of Gab1^{WT} overexpression on IGF-I-induced myogenic differentiation (Fig. 9, *C* and *D*). These findings suggest that Gab1 inhibits IGF-I-dependent myogenesis through activating MEK1/2-ERK1/2 pathway.

Finally, we examined the effect of adenoviral overexpression of constitutively active MEK1 (MEK1^{CA}). Overexpression of MEK1^{CA} repressed the enhanced myogenic differentiation observed in myoblasts overexpressing Gab1$^{\Delta SHP2}$ (Fig. 10, *A* and *B*). Collectively, interaction of Gab1 with SHP2 negatively regulates IGF-I-dependent myogenic differentiation in C2C12 myoblasts via activation of the MEK1/2-ERK1/2 pathway (Fig. 11).

DISCUSSION

In this study, we investigated the role of Gab1 in skeletal muscle differentiation. To our knowledge, this study demon-

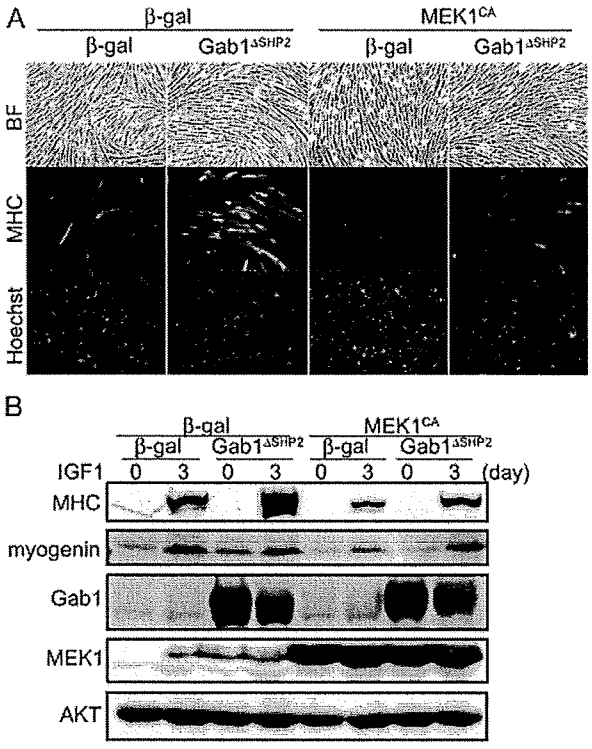

FIGURE 10. **Overexpression of constitutively active MEK1 abrogates the promoting effect of Gab1$^{\Delta SHP2}$ on myogenic differentiation in C2C12 cells.** *A*, C2C12 myoblasts were subjected to dual infection of adenovirus vectors expressing either β-gal or constitutively active MEK1 (MEK1^{CA}) with Gab1$^{\Delta SHP2}$. On the third day after myogenic induction, the cells were immunostained with anti-MHC antibody and post-stained with Hoechst 33342 nuclear dye. Overexpression of MEK1^{CA} in C2C12 significantly repressed the promoting effect of the overexpression of Gab1$^{\Delta SHP2}$ on IGF-I-induced myogenic differentiation. *B*, C2C12 myoblasts were subjected to dual infection of adenovirus vectors similar to *A*. The cell lysates were collected from 3.5-cm dishes and subjected to Western blot analysis. Dual overexpression of MEK1^{CA} with Gab1$^{\Delta SHP2}$ repressed the promoting effect of Gab1$^{\Delta SHP2}$ on the induction of MHC protein. Experiments were repeated three times with similar results.

strates for the first time that Gab1 has an inhibitory role in IGF-I-induced myogenic differentiation through activating SHP2-MEK1/2-ERK1/2 signaling pathway.

IGF-I induced complex formation of Gab1 with SHP2 in C2C12 myoblasts. It has been reported that Gab1 undergoes dramatic tyrosine-dephosphorylation upon changing growth medium to differentiation medium containing 2% HS in C2C12 cells (42). This finding indicated that Gab1 might have a key role in myogenic differentiation. Recently, it has been reported that Gab1 itself is a substrate of SHP2 (39). Furthermore, it has been reported that phosphorylation of ERK1/2 decreases while phosphorylation of AKT increases during differentiation with either insulin or 2% HS (9). Therefore, tyrosine dephosphorylation of Gab1 and subsequent dissociation of SHP2 from dephosphorylated Gab1 might be essential steps for the diminution of ERK1/2 activity during myogenic differentiation.

The Gab1-SHP2 complex formation is indispensable for IGF-I-induced activation of ERK1/2. It has been reported that Gab1-SHP2 interaction has an essential role for ERK1/2 activation downstream of EGF family/ErbB receptor signaling or hepatocyte growth factor/c-Met signaling (20–23). Furthermore, the recent study creating liver-specific Gab1 knock-out mice

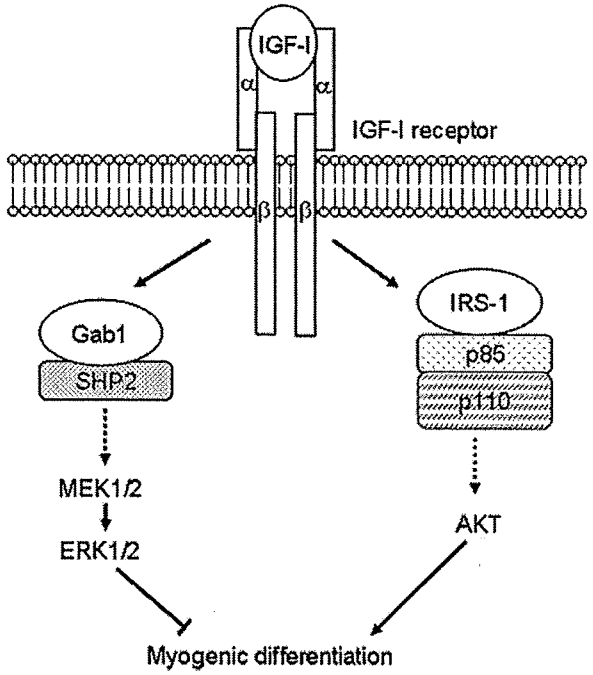

FIGURE 11. **Schematic models of the roles of Gab1 in IGF-I-dependent myogenic differentiation.** IGF-I induces tyrosine phosphorylation of Gab1 and subsequent association of Gab1 with SHP2. Gab1-SHP2 complex plays a critical role in activation of ERK1/2 in C2C12 myoblasts. Furthermore, Gab1-SHP2 complex negatively regulates myogenic differentiation via activation of MEK1/2-ERK1/2 pathway. On the other hand, IGF-I stimulation also induced tyrosine phosphorylation of IRS-I and subsequent association with p85 PI3K subunit. IRS-I-p85 complex formation has been reported to be indispensable for PI3K-AKT signaling, which might result in promotion of myogenic differentiation.

also demonstrated that Gab1 is required for both insulin-elicited ERK1/2 activation and subsequent inhibition of IRS-1-PI3K-AKT signaling (34). Here, we demonstrated that overexpression of Gab1$^{\Delta SHP2}$, which is incapable of associating with SHP2, repressed IGF-I-dependent activation of ERK1/2 in C2C12 myoblasts. In a similar context, SHP2 itself has been reported to have crucial roles for ERK1/2 activation downstream of various growth factors, including IGF-I (24, 43–46). We also observed that overexpression of phosphatase-inactive SHP2 (SHP2$^{C/S}$) inhibited IGF-I-dependent activation of ERK1/2 in C2C12 myoblasts. These findings demonstrate that Gab1-SHP2 complex formation is requisite for both activation of SHP2 itself and ERK1/2 upon IGF-1 stimulation in C2C12 myoblasts. Because the mechanism how SHP2 regulates receptor tyrosine kinase-mediated ERK1/2 activation remains controversial (18, 19), further analyses are needed for uncovering the mechanism how Gab1-SHP2 complex regulates IGF-I-induced activation of ERK1/2.

The Gab1-SHP2 complex exerts an inhibitory effect on the IGF-I-induced myogenic differentiation through activation of ERK1/2. IGFs have been reported to stimulate both proliferation and differentiation of skeletal muscle cells in culture (3, 4). IGFs activate two major cytoplasmic signaling pathways, PI3K-AKT cascade and Raf-MEK1/2-ERK1/2 MAPK cascade. The former has been reported to have positive effects on myogenesis, and the latter MAPK-signaling cascade has been reported to have detrimental effects on the myogenic differentiation

induced by insulin or IGFs (3, 9, 10). SHP2 has been also reported to play an inhibitory role for myogenic differentiation in the presence of fibroblast growth factor 2 (FGF2) in C2C12 myoblasts partly in an ERK1/2-dependent manner (44). We found that IGF-I-induced myogenic differentiation was inhibited by overexpression of either $Gab1^{WT}$ or $Gab1^{\Delta p85}$, but not by that of $SHP2^{WT}$. In addition, IGF-I-induced ERK1/2 activation in C2C12 myoblasts was enhanced by overexpression of either $Gab1^{WT}$ or $Gab1^{\Delta p85}$, but not by that of $SHP2^{WT}$. SHP2 can be specifically activated through binding directly with tyrosine-phosphorylated docking proteins such as Gab1 or FRS2α (18), suggesting that a sufficient amount of Gab1 is required to fully activate SHP2 by binding with SHP2 and that an insufficient amount of endogenous Gab1 might be the major limiting factor in overexpressed $SHP2^{WT}$-mediated myogenic differentiation. Collectively, these data suggest that Gab1 is a crucial negative regulator for IGF-I-dependent myogenic differentiation through activation of the SHP2-MEK1/2-ERK1/2 signaling pathway (Fig. 10).

The migration of muscle progenitor cells into the limb anlage from somites is strongly impaired in Gab1-knock-out embryos similarly in c-Met-knock-out mice (32). Furthermore, it has been reported that the knock-in mice, which carry mutant Gab1 incapable of binding with SHP2, displayed quite similar defects in migration of muscle progenitor cells from somites into the limb anlage during embryogenesis as observed in Gab1-knock-out mice (29). In clear contrast, the knock-in mice, which carry mutant Gab1 incapable of binding either Grb2 or c-Met, did not show any defects in migration of muscle progenitor cells, suggesting the specific role of Gab1-SHP2 complex in the migration of muscle progenitor cells (29). These previous data coincide with our findings that Gab1-SHP2 interaction has an inhibitory effect on IGF-I-induced myogenic differentiation. Taken together, Gab1 might play a key role not only for inhibition of myogenesis but also for maintenance of the undifferentiated state of mesenchymal cells through activation of SHP2.

Although the PI3K-AKT signaling pathway is central to IGF-I-dependent signaling and myogenic differentiation, our data demonstrate that the diminution of ERK1/2 activity is a prerequisite for IGF-I-induced myogenesis. IGFs promote skeletal muscle differentiation through PI3K-AKT-dependent signaling pathway (3, 6, 7, 47–49). It has been reported that the activity of AKT increased during myogenic differentiation under cultivation in 2% HS or IGF-I-containing differentiation medium (9). We found that overexpression of $Gab1^{\Delta p85}$ in C2C12 myoblasts resulted in enhanced activation of AKT upon stimulation with IGF-I, compared with those overexpressing $Gab1^{WT}$ or $Gab1^{\Delta SHP2}$. However, overexpression of $Gab1^{\Delta p85}$ did not enhance, but repressed IGF-I-induced myogenic differentiation to a similar extent to $Gab1^{WT}$. In clear contrast, overexpression of $Gab1^{\Delta SHP2}$ significantly enhanced IGF-I-induced myogenic differentiation compared with control. These findings indicate that myogenic differentiation requires the diminution of Gab1-SHP2-ERK1/2 signaling pathway prior to full activation of PI3K-AKT signaling pathway. It has been reported that the blockade of ERK1/2 signaling pathway enhances myogenic differentiation (3, 8–10). Inhibition of the ERK1/2 pathway has been reported to up-regulate Mirk/dyrk1B, a RhoA-dependent serine/threonine kinase that positively regulates skeletal muscle differentiation and inhibits apoptosis of myoblasts (50). Mirk/dyrk1B might be one of the candidate molecules through which ERK1/2 exerts an inhibitory effect on skeletal muscle differentiation.

In conclusion, the present study reveals that Gab1-SHP2 interaction exerts an inhibitory effect on IGF-I-dependent myogenic differentiation via activation of ERK1/2 signaling pathway.

Acknowledgments—We are grateful to S. Kawashima (Kobe University) for adenovirus vectors expressing dominant-negative MEK1 ($MEK1^{DN}$) and constitutively active MEK1 ($MEK1^{CA}$); T. Saito and S. Yamasaki (RIKEN Research Center for Allergy and Immunology) for $Gab2^{\Delta SHP2}$ cDNA; J. T. Pearson for his critical reading of this manuscript; Yuko Matsuura and Masako Suto for secretarial work; and Maki Yoshida, Y Mizushima, and Manami Sone for their technical assistance.

REFERENCES

1. Bach, L. A., Salemi, R., and Leeding, K. S. (1995) *Endocrinology* **136**, 5061–5069
2. Ewton, D. Z., Roof, S. L., Magri, K. A., McWade, F. J., and Florini, J. R. (1994) *J. Cell Physiol.* **161**, 277–284
3. Coolican, S. A., Samuel, D. S., Ewton, D. Z., McWade, F. J., and Florini, J. R. (1997) *J. Biol. Chem.* **272**, 6653–6662
4. Florini, J. R., Ewton, D. Z., and Coolican, S. A. (1996) *Endocr. Rev.* **17**, 481–517
5. White, M. F. (2003) *Science* **302**, 1710–1711
6. Kaliman, P., Vinals, F., Testar, X., Palacin, M., and Zorzano, A. (1996) *J. Biol. Chem.* **271**, 19146–19151
7. Kaliman, P., Canicio, J., Shepherd, P. R., Beeton, C. A., Testar, X., Palacin, M., and Zorzano, A. (1998) *Mol. Endocrinol.* **12**, 66–77
8. Bennett, A. M., and Tonks, N. K. (1997) *Science* **278**, 1288–1291
9. de Alvaro, C., Martinez, N., Rojas, J. M., and Lorenzo, M. (2005) *Mol. Biol. Cell* **16**, 4454–4461
10. Tortorella, L. L., Milasincic, D. J., and Pilch, P. F. (2001) *J. Biol. Chem.* **276**, 13709–13717
11. Gu, H., and Neel, B. G. (2003) *Trends Cell Biol.* **13**, 122–130
12. Nishida, K., and Hirano, T. (2003) *Cancer Sci.* **94**, 1029–1033
13. Holgado-Madruga, M., Emlet, D. R., Moscatello, D. K., Godwin, A. K., and Wong, A. J. (1996) *Nature* **379**, 560–564
14. Montagner, A., Yart, A., Dance, M., Perret, B., Salles, J. P., and Raynal, P. (2005) *J. Biol. Chem.* **280**, 5350–5360
15. Nishida, K., Yoshida, Y., Itoh, M., Fukada, T., Ohtani, T., Shirogane, T., Atsumi, T., Takahashi-Tezuka, M., Ishihara, K., Hibi, M., and Hirano, T. (1999) *Blood* **93**, 1809–1816
16. Takahashi-Tezuka, M., Yoshida, Y., Fukada, T., Ohtani, T., Yamanaka, Y., Nishida, K., Nakajima, K., Hibi, M., and Hirano, T. (1998) *Mol. Cell Biol.* **18**, 4109–4117
17. Weidner, K. M., Di Cesare, S., Sachs, M., Brinkmann, V., Behrens, J., and Birchmeier, W. (1996) *Nature* **384**, 173–176
18. Neel, B. G., Gu, H., and Pao, L. (2003) *Trends Biochem. Sci.* **28**, 284–293
19. Tiganis, T., and Bennett, A. M. (2007) *Biochem. J.* **402**, 1–15
20. Cunnick, J. M., Dorsey, J. F., Munoz-Antonia, T., Mei, L., and Wu, J. (2000) *J. Biol. Chem.* **275**, 13842–13848
21. Cunnick, J. M., Mei, L., Doupnik, C. A., and Wu, J. (2001) *J. Biol. Chem.* **276**, 24380–24387
22. Nakaoka, Y., Nishida, K., Fujio, Y., Izumi, M., Terai, K., Oshima, Y., Sugiyama, S., Matsuda, S., Koyasu, S., Yamauchi-Takihara, K., Hirano, T., Kawase, I., and Hirota, H. (2003) *Circ. Res.* **93**, 221–229
23. Schaeper, U., Gehring, N. H., Fuchs, K. P., Sachs, M., Kempkes, B., and Birchmeier, W. (2000) *J. Cell Biol.* **149**, 1419–1432

24. Cunnick, J. M., Meng, S., Ren, Y., Desponts, C., Wang, H. G., Djeu, J. Y., and Wu, J. (2002) *J. Biol. Chem.* **277,** 9498–9504
25. Dance, M., Montagner, A., Yart, A., Masri, B., Audigier, Y., Perret, B., Salles, J. P., and Raynal, P. (2006) *J. Biol. Chem.* **281,** 23285–23295
26. Jin, Z. G., Wong, C., Wu, J., and Berk, B. C. (2005) *J. Biol. Chem.* **280,** 12305–12309
27. Laramee, M., Chabot, C., Cloutier, M., Stenne, R., Holgado-Madruga, M., Wong, A. J., and Royal, I. (2007) *J. Biol. Chem.* **282,** 7758–7769
28. Mattoon, D. R., Lamothe, B., Lax, I., and Schlessinger, J. (2004) *BMC. Biol.* **2,** 24
29. Schaeper, U., Vogel, R., Chmielowiec, J., Huelsken, J., Rosario, M., and Birchmeier, W. (2007) *Proc. Natl. Acad. Sci. U. S. A.* **104,** 15376–15381
30. Rodrigues, G. A., Falasca, M., Zhang, Z., Ong, S. H., and Schlessinger, J. (2000) *Mol. Cell Biol.* **20,** 1448–1459
31. Itoh, M., Yoshida, Y., Nishida, K., Narimatsu, M., Hibi, M., and Hirano, T. (2000) *Mol. Cell Biol.* **20,** 3695–3704
32. Sachs, M., Brohmann, H., Zechner, D., Muller, T., Hulsken, J., Walther, I., Schaeper, U., Birchmeier, C., and Birchmeier, W. (2000) *J. Cell Biol.* **150,** 1375–1384
33. Nakaoka, Y., Nishida, K., Narimatsu, M., Kamiya, A., Minami, T., Sawa, H., Okawa, K., Fujio, Y., Koyama, T., Maeda, M., Sone, M., Yamasaki, S., Arai, Y., Koh, G. Y., Kodama, T., Hirota, H., Otsu, K., Hirano, T., and Mochizuki, N. (2007) *J. Clin. Invest.* **117,** 1771–1781
34. Bard-Chapeau, E. A., Hevener, A. L., Long, S., Zhang, E. E., Olefsky, J. M., and Feng, G. S. (2005) *Nat. Med.* **11,** 567–571
35. Yamasaki, S., Nishida, K., Yoshida, Y., Itoh, M., Hibi, M., and Hirano, T. (2003) *Oncogene* **22,** 1546–1556
36. Becker, T. C., Noel, R. J., Coats, W. S., Gomez-Foix, A. M., Alam, T., Gerard, R. D., and Newgard, C. B. (1994) *Methods Cell Biol.* **43,** 161–189
37. Ueyama, T., Kawashima, S., Sakoda, T., Rikitake, Y., Ishida, T., Kawai, M., Yamashita, T., Ishido, S., Hotta, H., and Yokoyama, M. (2000) *J. Mol. Cell Cardiol.* **32,** 947–960
38. Sarbassov, D. D., and Peterson, C. A. (1998) *Mol. Endocrinol.* **12,** 1870–1878
39. Zhang, S. Q., Tsiaras, W. G., Araki, T., Wen, G., Minichiello, L., Klein, R., and Neel, B. G. (2002) *Mol. Cell Biol.* **22,** 4062–4072
40. Meng, S., Chen, Z., Munoz-Antonia, T., and Wu, J. (2005) *Biochem. J.* **391,** 143–151
41. Yamasaki, S., Nishida, K., Hibi, M., Sakuma, M., Shiina, R., Takeuchi, A., Ohnishi, H., Hirano, T., and Saito, T. (2001) *J. Biol. Chem.* **276,** 45175–45183
42. Kontaridis, M. I., Liu, X., Zhang, L., and Bennett, A. M. (2001) *J. Cell Sci.* **114,** 2187–2198
43. Ivins, Z. C., Kontaridis, M. I., Fornaro, M., Feng, G. S., and Bennett, A. M. (2004) *J. Cell Physiol.* **199,** 227–236
44. Kontaridis, M. I., Liu, X., Zhang, L., and Bennett, A. M. (2002) *Mol. Cell Biol.* **22,** 3875–3891
45. Shi, Z. Q., Yu, D. H., Park, M., Marshall, M., and Feng, G. S. (2000) *Mol. Cell Biol.* **20,** 1526–1536
46. Shi, Z. Q., Lu, W., and Feng, G. S. (1998) *J. Biol. Chem.* **273,** 4904–4908
47. Jiang, B. H., Zheng, J. Z., Aoki, M., and Vogt, P. K. (2000) *Proc. Natl. Acad. Sci. U. S. A.* **97,** 1749–1753
48. Jiang, B. H., Zheng, J. Z., and Vogt, P. K. (1998) *Proc. Natl. Acad. Sci. U. S. A.* **95,** 14179–14183
49. Jiang, B. H., Aoki, M., Zheng, J. Z., Li, J., and Vogt, P. K. (1999) *Proc. Natl. Acad. Sci. U. S. A.* **96,** 2077–2081
50. Deng, X., Ewton, D. Z., Pawlikowski, B., Maimone, M., and Friedman, E. (2003) *J. Biol. Chem.* **278,** 41347–41354

The EMBO Journal (2008) 27, 522–534 | © 2008 European Molecular Biology Organization | All Rights Reserved 0261-4189/08
www.embojournal.org

THE EMBO JOURNAL

Spatial and temporal role of the apelin/APJ system in the caliber size regulation of blood vessels during angiogenesis

Hiroyasu Kidoya[1], Masaya Ueno[1], Yoshihiro Yamada[1], Naoki Mochizuki[2], Mitsugu Nakata[3], Takashi Yano[3], Ryo Fujii[4] and Nobuyuki Takakura[1,*]

[1]Department of Signal Transduction, Research Institute for Microbial Diseases, Osaka University, Suita, Osaka, Japan, [2]Department of Structural Analysis, National Cardiovascular Center Research Institute, Suita, Osaka, Japan, [3]Pharmaceutical Research Laboratories 1, Pharmaceutical Research Division, Takeda Pharmaceutical Company Limited, Yodogawa, Osaka, Japan and [4]Frontier Research Laboratories, Pharmaceutical Research Division, Takeda Pharmaceutical Company Limited, Tsukuba-shi, Ibaraki, Japan

Blood vessels change their caliber to adapt to the demands of tissues or organs for oxygen and nutrients. This event is mainly organized at the capillary level and requires a size-sensing mechanism. However, the molecular regulatory mechanism involved in caliber size modification in blood vessels is not clear. Here we show that apelin, a protein secreted from endothelial cells under the activation of Tie2 receptor tyrosine kinase on endothelial cells, plays a role in the regulation of caliber size of blood vessel through its cognate receptor APJ, which is expressed on endothelial cells. During early embryogenesis, APJ is expressed on endothelial cells of the new blood vessels sprouted from the dorsal aorta, but not on pre-existing endothelial cells of the dorsal aorta. Apelin-deficient mice showed narrow blood vessels in intersomitic vessels during embryogenesis. Apelin enhanced endothelial cell proliferation in the presence of vascular endothelial growth factor and promoted cell-to-cell aggregation. These results indicated that the apelin/APJ system is involved in the regulation of blood vessel diameter during angiogenesis.

The EMBO Journal (2008) **27**, 522–534. doi:10.1038/sj.emboj.7601982; Published online 17 January 2008
Subject Categories: development
Keywords: angiogenesis; angiopoietin-1; apelin; APJ; lumen size

Introduction

The vascular system of vertebrates has a highly organized and hierarchical structure, ranging from large blood vessels down to finely sized capillaries. The intraluminal cavity of blood vessels is lined almost exclusively with endothelial cells (ECs). The formation of blood vessels is initiated by the assembly and tube formation of ECs, or EC progenitors. This process is termed vasculogenesis and is followed by angiogenesis, which results in the emergence of new vessels through sprouting and elongation from, or the remodelling of, pre-existing vessels (Risau, 1997).

Many genes involved in these processes have been isolated and their roles in the specification of vascular lineage from mesodermal cells and vascular morphogenesis have been analysed (Wang *et al*, 1998; Adams *et al*, 1999; Gale and Yancopoulos, 1999; Oettgen, 2001; Zhong *et al*, 2001; Carmeliet, 2003; Gerhardt and Betsholtz, 2003; Simon, 2004). Among many molecules, vascular endothelial growth factors (VEGFs) and their cognate receptors (VEGFRs) play central roles in the differentiation (arterial), proliferation, migration and survival of ECs in physiological and pathological conditions (Ferrara *et al*, 2003). Based on the diverse functions of VEGFs in blood vessel formation, the VEGF/VEGFR system has proved effective in the clinical management of cancer patients by negatively regulating angiogenesis (Ferrara and Alitalo, 1999; Jain, 2005). Therefore, these results indicate the importance of developmental studies for understanding blood vessel formation.

In the maturation process involved in blood vessel formation, the ECs, which form the tube, recruit supporting mural cells (MCs) such as periendothelial cells (pericytes) or vascular smooth muscle cells, by releasing platelet-derived growth factor (PDGF)-BB (Lindahl *et al*, 1997). MCs subsequently adhere to ECs resulting in the formation of a structurally stable blood vessel. It has been proposed that this cell adhesion between ECs and MCs is induced when angiopoietin 1 (Ang1), produced from MCs, stimulates Tie2, a receptor tyrosine kinase on ECs (Dumont *et al*, 1994; Sato *et al*, 1995; Suri *et al*, 1996).

During angiogenesis, blood vessels need to be able to adjust their caliber, in order to allow them to respond adequately to the changes in demand for oxygen and nutrients made by the organs and tissues. This caliber adjustment is involved in the maturation process during angiogenesis; however, the molecular mechanism involved in the determination of blood vessel size has not been elucidated. A potent regulator of the enlargement of blood vessel caliber is the Ang1/Tie2 system, because transgenic overexpression of Ang1 in the keratinocyte-induced enlarged blood vessels in the dermis (Suri *et al*, 1998) and administration of a potent Ang1 variant were also reported to induce enlargement of blood vessels (Cho *et al*, 2005; Thurston *et al*, 2005). Therefore, the analysis of the precise molecular mechanism of how the Ang1/Tie2 system induces enlargement of blood vessels would allow us to understand the process of determination of blood vessel size during angiogenesis.

In this report, by the analysis of downstream signalling of Ang1/Tie2 in ECs, we found that apelin, a recently isolated bioactive peptide from bovine gastric extract working as a

*Corresponding author. Department of Signal Transduction, Research Institute for Microbial Diseases, Osaka University, 3-1 Yamadaoka, Suita, Osaka 565-0871, Japan. Tel.: +81 6 6879 8316; Fax: +81 6 6879 8314; E-mail: ntakaku@biken.osaka-u.ac.jp

Received: 19 April 2007; accepted: 18 December 2007; published online: 17 January 2008

ligand for APJ, is upregulated by Ang1 stimulation of human umbilical vein endothelial cells (HUVECs). A sequence of apelin cDNA encodes a protein of 77 amino acids, which can generate two active polypeptides: the long (42–77) and the short (65–77) forms of apelin (Tatemoto *et al*, 1998; Kawamata *et al*, 2001; Masri *et al*, 2005). Both forms activate APJ.

APJ is a G protein-coupled receptor, which has been reported to be expressed in the cardiovascular and central nervous systems (O'Dowd *et al*, 1993; Devic *et al*, 1999). In brain tissues, APJ expression is observed in neurons (Edinger *et al*, 1998) as well as in oligodendrocytes and astrocytes (Croitoru-Lamoury *et al*, 2003). In the brain, the apelin/APJ system plays a role in maintaining body fluid homeostasis and regulating the release of vasopressin from the hypothalamus (De Mota *et al*, 2004). In the cardiovascular system, APJ is expressed in an endothelial lineage in various species such as amphibian, mouse and human (Devic *et al*, 1996, 1999; Katugampola *et al*, 2001). In the mouse and human, the expression of the receptor has also been detected by immunocytochemistry in vascular smooth muscle cells and cardiomyocytes (Kleinz and Davenport, 2004). Apelin/APJ function in cardiomyocytes is thought to be associated with a very strong inotropic activity (Szokodi *et al*, 2002; Ashley *et al*, 2005). The function of apelin/APJ in EC lineage is reported to be associated with the hypotensive activity of apelin (Ishida *et al*, 2004), as the activation of APJ leads to nitric oxide (NO) production by the ECs (Tatemoto *et al*, 2001), and this possibly plays a role in the relaxation of smooth muscle cells.

Using the morpholino antisense oligonucleotide, requisite roles of the apelin/APJ system have been reported in the cardiovascular system of *Xenopus laevis* (Cox *et al*, 2006; Inui *et al*, 2006) and zebrafish (Scott *et al*, 2007). *Xenopus apelin* (*Xapelin*) was detected in the region around the presumptive blood vessels during early embryogenesis and overlapped with the expression of *Xmsr*, the *Xenopus* homolog of *APJ*. Overexpression of *Xapelin* disorganized the expression of the endothelial precursor cell marker *XlFli* at the neurula stage. Knockdown of *Xapelin* or Xmsr induced abnormal heart morphology and attenuated the expression of *Tie2*, resulting in the disruption of blood vessel formation in the posterior cardinal vein, intersomitic vessels (ISVs) and vitelline vessels. By contrast, apelin protein has been shown to induce angiogenesis in the chicken chorioallantoic membrane assay (Cox *et al*, 2006). Although the involvement of apelin/APJ in angiogenesis and the regulation of proliferation of ECs has been suggested, the precise function of apelin/APJ in the morphology of blood vessels in mammals is not clear.

Here, using various *in vitro* and *in vivo* assays, we show that apelin induces enlargement of blood vessels. Moreover, the physiological function of apelin has been studied through the generation of apelin-mutant mice and the relationship of Ang1/Tie2 signalling to apelin has been studied by mating apelin-mutant mice with Ang1 transgenic mice. Finally, using the para-aortic splanchnopleural mesoderm (P-Sp) organ culture system that mimics *in vivo* vasculogenesis and angiogenesis and various *in vitro* HUVEC culture systems, we have studied how apelin regulates the enlargement of blood vessels.

Results

Ang1 induces apelin expression on ECs

To elucidate the molecular mechanism by which Tie2 regulates the caliber change of blood vessels from small to larger ones, and in order to isolate the genes encoding proteins that are involved in caliber change and specifically expressed in HUVECs stimulated by Ang1, we constructed a subtraction library from HUVECs with Tie2 stimulated by Ang1 as a tester, and HUVECs with no stimulation of Tie2 as the driver (Figure 1A). One of these isolated cDNA clones was the human gene encoding apelin (Figure 1B–D). Real-time polymerase chain reaction (PCR) analysis revealed that apelin mRNA was potently increased in HUVECs after stimulation by Ang1 in a time-dependent manner (Figure 1B) and we confirmed that the expression of apelin protein was markedly upregulated on HUVECs stimulated by Ang1 (Figure 1C). Moreover, the dose-dependent effect of Ang1 on apelin production from HUVECs was confirmed by enzyme immunoassay, using the culture supernatant of HUVECs (Figure 1D).

In order to confirm further the upregulation of apelin in ECs *in vivo*, we analysed apelin expression in the dermis of Ang1 transgenic (Ang1Tg) mice, in which Ang1 was overexpressed in the keratinocytes under the transcriptional control of K14 promoter (Suri *et al*, 1998). As shown in Figure 1E, apelin expression on ECs in the dermis at postnatal day 7 was increased in Ang1Tg mice compared to that in wild-type (WT) mice. We confirmed the overexpression of apelin mRNA in Ang1Tg mice by quantitative real-time RT–PCR using ECs fractionated from the dermis by a cell sorter (Figure 1F). As it is well known that Ang1 is involved in angiogenesis, next we observed the effect of other proangiogenic molecules on the expression of apelin on ECs. bFGF induced apelin expression on HUVECs; however, VEGF, PDGF-BB or EGF did not affect apelin expression (Supplementary Figure 1A and B).

Apelin with VEGF induces proliferation of ECs

With respect to the enlargement of blood vessels, it seems likely that apelin causes the proliferation of ECs. To test this ability, firstly we studied the proliferation of ECs using HUVECs. As shown in Figure 2A, apelin was not effective in inducing proliferation of HUVECs. However, upon stimulation with VEGF, the expression level of APJ was upregulated in HUVECs, at both the mRNA and protein levels (Figure 2B–D and Supplementary Figure 2). Cell surface expression of APJ on HUVECs was confirmed by both cell surface biotinylation experiment (Figure 2D) and confocal laser scanning analysis (Supplementary Figure 2). Consistent with this result, VEGF-induced proliferation of HUVECs was enhanced by the addition of apelin in a dose-dependent manner (Figure 2A). Among proangiogenic cytokines, such as Ang1, EGF, bFGF, PDGF-BB and VEGF, only VEGF induced APJ expression on HUVECs (Figure 2B–D and Supplementary Figure 1C and D).

These results suggested that APJ is expressed and affects ECs during angiogenesis in which VEGF levels are upregulated. Next we observed the proliferation of primary ECs from the culture of the AGM region (aorta–gonad–mesonephros region followed by P-Sp region at embryonic day (E) 10.5 to E11.5) in which angiogenesis was actively taking place. APJ was highly expressed in the AGM region compared to other tissues, such as E10.5 yolk sac, head region and heart, and adult heart (Figure 3A). Furthermore, APJ was expressed strongly in $CD45^{-}CD31^{+}$ ECs from the AGM region compared to those from E10.5 heart and adult heart. Although ECs in E10.5 yolk sac and head region expressed APJ, the

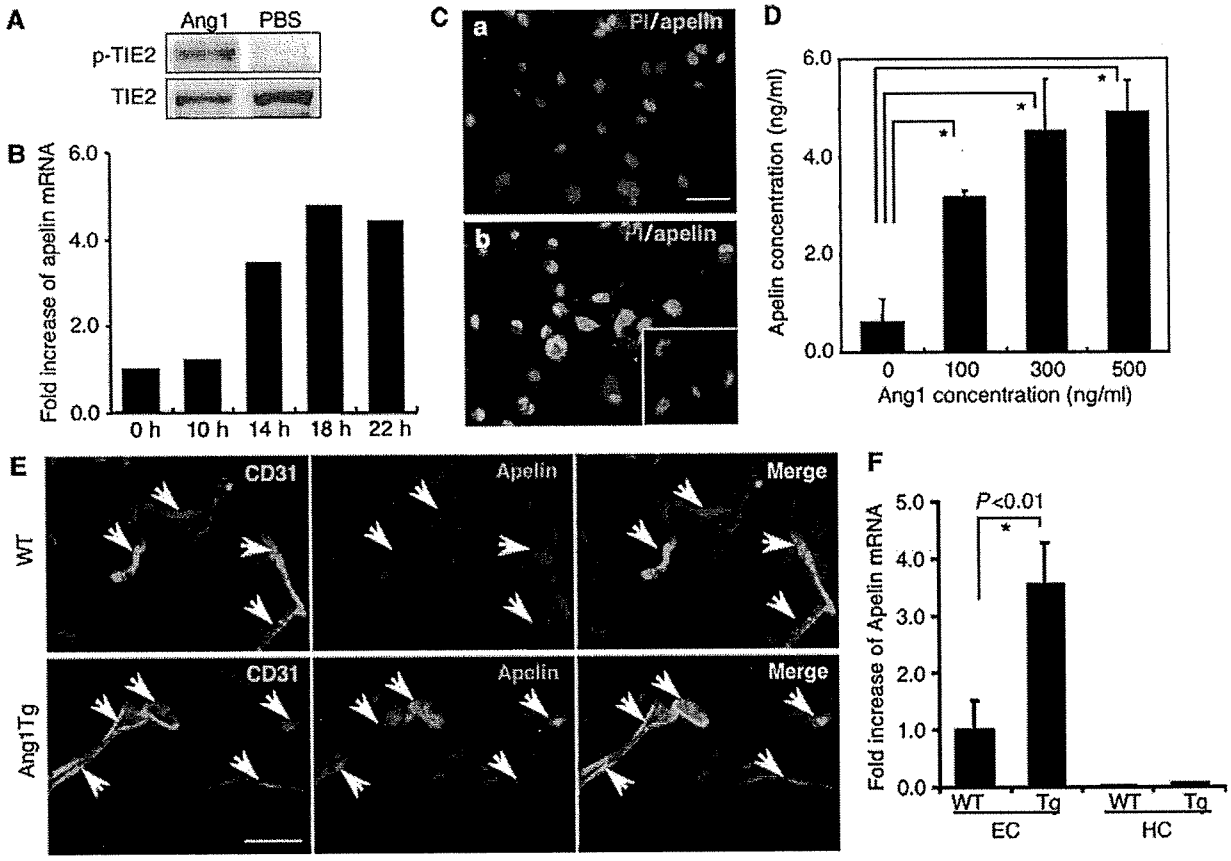

Figure 1 Ang1 stimulation induces apelin expression in ECs *in vitro* and *in vivo*. (**A**) Tie2 phosphorylation on HUVECs by Ang1 in our system. HUVECs, serum-starved for 2 h, were either treated or not treated with 500 ng/ml Ang1 for 10 min. Phosphorylation was studied by immunoblotting using phosphospecific antibody (p-Tie2). (**B**) Quantitative real-time RT–PCR analysis of apelin mRNA in HUVECs. Total RNA was extracted from HUVECs that had been stimulated with Ang1 for 0–22 h. Results are shown as fold increase in comparison with basal levels of HUVECs (0 h). (**C**) Immunocytochemical analysis of apelin expression in HUVECs, non-stimulated (a) and stimulated (b) by Ang1 (500 ng/ml) for 20 h. Cells were stained with anti-apelin mAb (green). The inset in (b) shows HUVECs stained with secondary antibody as a negative control. Nuclei were stained with propidium iodide (PI; red). Scale bar indicates 50 μm. (**D**) Quantitative enzyme immunoassay of apelin production from HUVECs stimulated by various doses of Ang1. $^*P<0.001$ ($n=3$). (**E**) Immunochemical detection of apelin peptide in the dermis. Sections of skin from WT and Ang1Tg neonatal mice were stained with anti-CD31 (green) and anti-apelin (red) mAb. Arrows indicate CD31$^+$ blood vessels. Scale bar indicates 30 μm. (**F**) Quantitative real-time RT–PCR analysis of apelin mRNA in ECs and hematopoietic cells (HCs) of Ang1Tg mice. RNA was prepared from sorted CD31$^+$CD45$^-$ ECs or CD31$^-$CD45$^+$ HCs from the dermis of WT or Ang1Tg neonatal mouse skin. $^*P<0.01$ ($n=3$).

expression level was weaker than that in the AGM region. When cells from the AGM region were cultured on apelin-expressing OP9 cells (Figure 3B), proliferation of CD45$^-$CD31$^+$ was increased compared with that on control OP9 cells and this proliferation by apelin was abrogated by the addition of anti-apelin blocking antibody (Figure 3C and D), suggesting that this action of proliferation by apelin is specific to the apelin/APJ system. Moreover, as APJ expression was weaker in ECs from adult heart (Figure 3A) or adult liver (data not shown) than in those from the AGM region, apelin did not induce proliferation of ECs in such adult tissues compared to those in the AGM region (Supplementary Figure 3).

Apelin induces the assembly of ECs

Although the proliferation of ECs is one of the factors involved in the construction of larger vessels, it is not the only one. The assembly or aggregation of ECs or endothelial progenitors, resulting in abundant cell-to-cell contact, is also necessary for the induction of a caliber change of blood vessels into larger ones. Therefore, next we tested the ability of apelin to regulate cell-to-cell contact. When cells from the AGM region were put on OP9 feeder cells, the control OP9 cells induced a cord-like structure of ECs, in contrast to the OP9 cells expressing apelin, which induced a sheet-like layer of ECs in abundance (Figure 4A and C). When cell-to-cell contact was observed using anti-VE-cadherin or -claudin5 antibodies, we confirmed that the sheet-like structure was composed of ECs connected with the junctional proteins, VE-cadherin (Figure 4B) or claudin5 (Supplementary Figure 4). Moreover, the addition of anti-apelin monoclonal antibody (mAb) inhibited the sheet-like layer formation of ECs induced by apelin (Figure 4B and Supplementary Figure 4). This sheet-like structure was already observed in the early stage of this culture (Figure 4C), suggesting that cell aggregation was initiated when ECs were seeded on OP9 cells expressing apelin.

Among many adhesion molecules tested, we found that the expression of the junctional protein, claudin5, was significantly induced by apelin on HUVECs, while that of VE-cadherin was only slightly induced, at both the mRNA

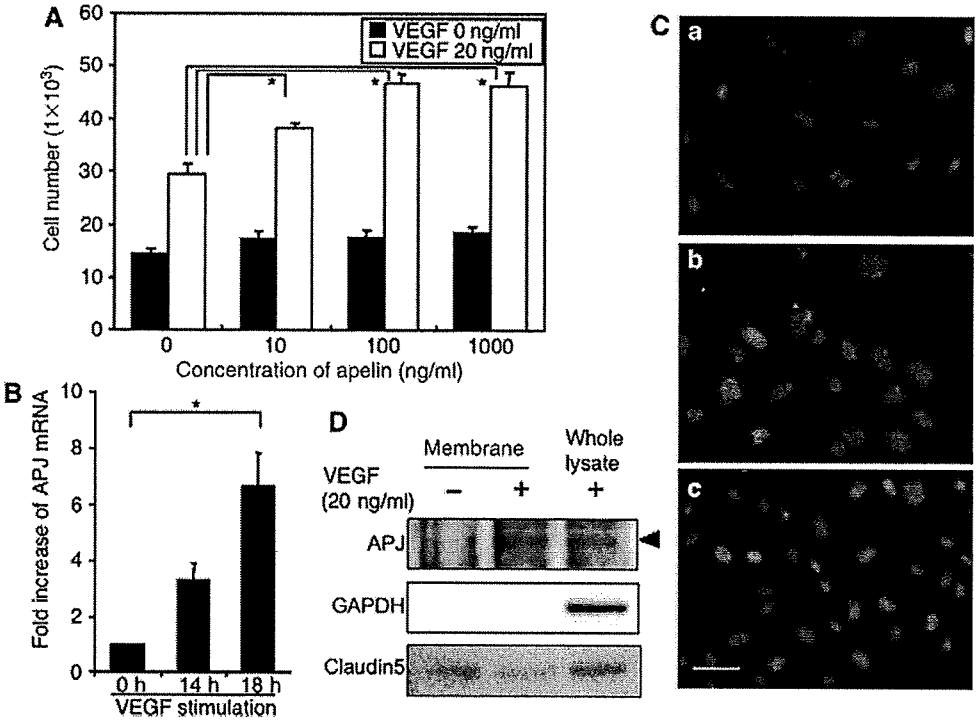

Figure 2 Apelin induces proliferation of HUVECs in a VEGF-dependent manner. (**A**) Proliferation of HUVECs by apelin. HUVECs (5×10^3) were cultured with apelin (0–1000 ng/ml) in the presence or absence of VEGF (20 ng/ml) for 48 h and the number of cells was counted. $^*P<0.001$ ($n=3$). (**B**) Quantitative real-time RT–PCR analysis of the induction of APJ expression by VEGF in HUVECs. HUVECs were stimulated with VEGF (10 ng/ml) for 0–18 h. Results are shown as fold increase in expression in comparison with levels in stimulated HUVECs at 0 h. $^*P<0.001$ ($n=3$). (**C**) APJ expression on HUVECs. HUVECs were cultured in the absence (a) or presence (b, c) of VEGF (20 ng/ml) for 24 h and stained with anti-APJ antibody (green) (a, b). (c) Cells stained with a secondary antibody alone as a negative control. Nuclei were stained with propidium iodide (red). Scale bar indicates 50 μm. (**D**) Western blot analysis of cell surface APJ expression on HUVECs that had been stimulated with VEGF (20 ng/ml) for 24 h. The purity of cell membrane protein was confirmed by the lack of intracellular protein GAPDH expression. Claudin5 expression was analysed for the experimental control of another cell surface protein. Note that the expression of a 60 kDa APJ protein was increased in HUVECs in the presence of VEGF.

and protein levels (Supplementary Figure 5). *In vitro* sheet-like formation of ECs and upregulation of cell-to-cell adhesion molecules by apelin indicated the involvement of the apelin/APJ system in the assembly of ECs. Next, we performed the cord formation assay of HUVECs on Matrigel in the presence or absence of apelin (Figure 5A). After 20 h of culture of HUVECs on Matrigel, they formed a cord-like structure in the absence of apelin (Figure 5Aa). However, in the presence of apelin, the HUVECs formed an enlarged cord-like structure (Figure 5Abd). In this assay, by using confocal laser scanning analysis, we confirmed that enlargement of this cord-like structure was induced by cell aggregation, but not by cell spreading (Supplementary Figure 6). This enlargement was completely blocked by anti-VE-cadherin blocking antibody (Figure 5Acd), suggesting that the enlarged cord-like formation induced by apelin was initiated by cell-to-cell contact. Moreover, in the spheroid assay (Korff and Augustin, 1998), HUVECs formed large spheroids in the presence of apelin (Figure 5B) and this action was abrogated by anti-apelin antibody. Therefore, these results strongly support the notion that the apelin/APJ system induces EC-to-EC assembly.

APJ expression in ECs during early embryogenesis

As APJ expression was observed in ECs during early embryogenesis (Figure 3), we studied which vessels expressed APJ in mouse embryos. At E8.5, cells committed into the endothelial lineage formed the dorsal aorta (DA), from which ECs started to sprout. As observed in Figure 6A, APJ expression was observed in those ECs that had sprouted from the DA but not in those that were forming the DA. At E9.5, APJ expression was observed in the migrating end region of ISVs sprouting from the DA (Figure 6B). Besides the expression of APJ in the ISVs, weak APJ expression was observed in the somites. These expression profiles were not very different from the results obtained by *in situ* hybridization analysis, as reported previously (Devic *et al*, 1999). In another area of the E9.5 embryo, we found that the anterior cardinal vein (ACV) expressed APJ. However, when compared to CD31 expression in ECs, APJ-positive ECs were observed in the migrating end of the ACV, but not in the base (Supplementary Figure 7). These expression profiles suggest that the apelin/APJ system may be associated with angiogenesis but not with vasculogenesis. Moreover, when apelin expression was observed in the somite region at E9.5, we found that apelin protein was detected in ISV (Supplementary Figure 8), suggesting that the apelin/APJ system may be associated with the formation of ISV.

Narrow blood vessels are induced in apelin-mutant mice

In order to understand the physiological function of apelin, we generated apelin-mutant mice (Supplementary Figure 9)

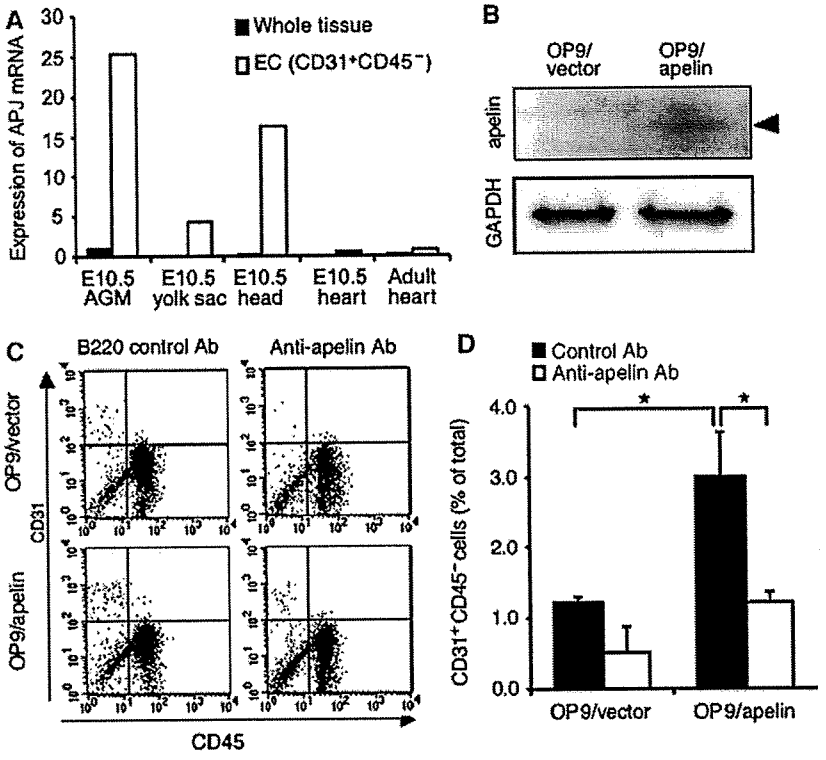

Figure 3 ECs from the AGM region express APJ and are induced to proliferate by apelin. (**A**) Quantitative real-time RT–PCR analysis of APJ expression in various tissues, as indicated. RNA from whole tissue, or $CD45^{-}CD31^{+}$ ECs sorted from various tissues, was evaluated for the expression of APJ. (**B**) Western blot analysis of apelin expression on OP9 cells induced by mock vector (OP9/vector) or apelin expression vector (OP9/apelin). An 8 kDa apelin protein was detected in OP9/apelin. GAPDH was used for the internal control. (**C**) Apelin-induced proliferation of ECs from E10.5 AGM region. Cells from the AGM region were cultured for 7 days, on an OP9/vector or OP9/apelin, in the presence or absence of anti-apelin or control B220 mAb. AGM cells harvested from cultures were stained with anti-CD31 and -CD45 mAbs and analysed by FACS. (**D**) Quantitative evaluation of the percentage of $CD31^{+}CD45^{-}$ vascular ECs cultured as described in (C). $^{*}P<0.001$ ($n=5$).

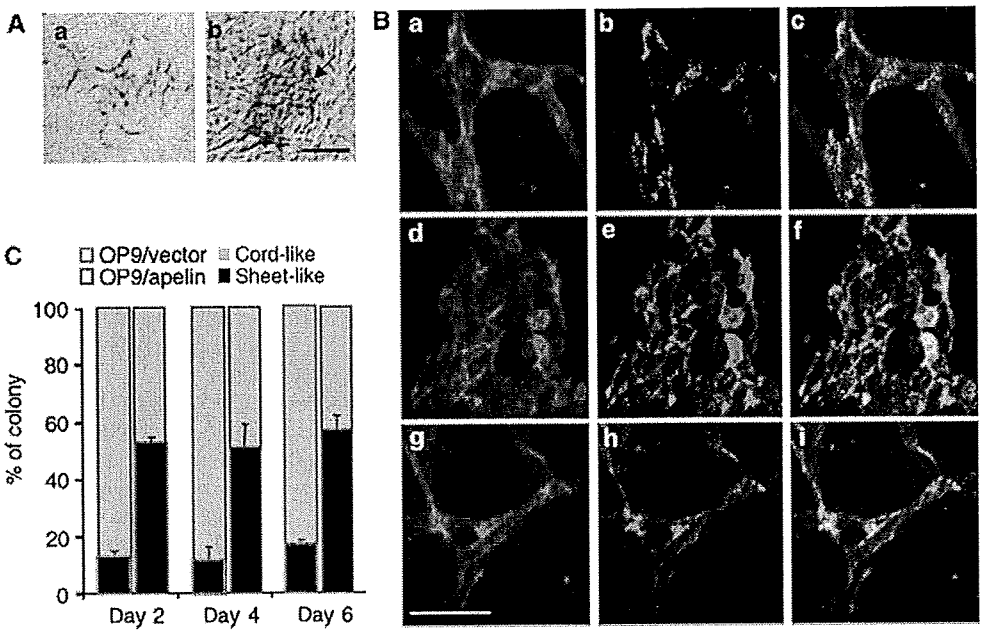

Figure 4 Endothelial sheet formation by apelin. (**A**) Cells from E11.5 AGM region were cocultured with an OP9/vector (a) or OP9/apelin (b) for 2–6 days, and CD31 immunostaining was performed. The arrow indicates the aggregated EC sheet. Scale bar indicates 100 μm. (**B**) Cells from E11.5 AGM region were cocultured for 6 days with an OP9/vector (a–c), OP9/apelin in the presence of B220 control antibody (d–f) or OP9/apelin in the presence of anti-apelin blocking antibody (g–i). ECs on OP9 cells were stained with anti-CD31 (a, d, g) and anti-VE-cadherin (b, e, h) antibodies. (c, f, i) Merged images of (a) and (b), (d) and (e), or (g) and (h), respectively. Scale bar indicates 50 μm. (**C**) The proportion of sheet-like or cord-like structures of ECs on OP9/apelin or OP9/vector stromal cells ($n=3$).

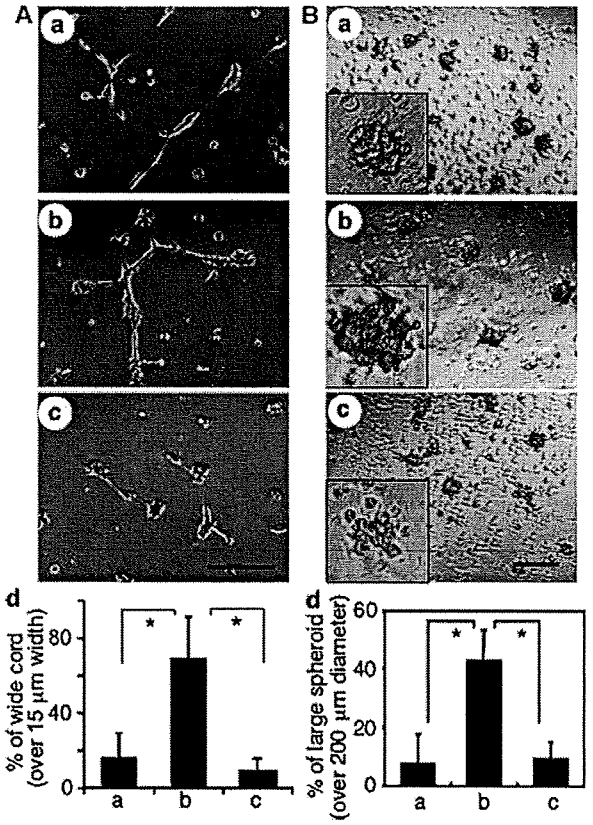

Figure 5 Morphological change of HUVECs stimulated with apelin. (A) Cord formation analysis of HUVECs cultured on Matrigel. HUVECs were cultured in the presence of VEGF (20 ng/ml) for 20 h, harvested, transferred onto Matrigel and cultured in the absence (a) or presence of apelin (b, c) for 10 h. Anti-VE-cadherin antibody (c) or control anti-B220 mAb (b) was added. Scale bar indicates 200 μm. (d) Quantitative evaluation of the width of the cord-like structure observed in the various culture conditions (a: control; b: apelin + anti-B220 mAb; c: apelin + anti- VE-cadherin antibody) described above. The percentage of wide cord (width >15 μm) among the total cord-like structure was calculated. $^*P<0.01$ ($n=3$). (B) HUVEC spheroid assay. HUVECs stimulated with VEGF for 24 h were harvested and cultured on nonadhesive dishes in the absence (a) or presence of apelin (b, c) for 10 h. Anti-apelin antibody (c) or control anti-B220 mAb (b) was added. Scale bar indicates 500 μm. The inset in each panel shows higher magnified representative spheroid under each condition. (d) Quantitative evaluation of the size of spheroid observed in the various culture conditions (a: control; b: apelin; c: apelin + anti-apelin antibody) described above. The percentage of large spheroid (diameter >200 μm) among the total spheroid was calculated. $^*P<0.01$ ($n=3$).

and observed blood vessel formation. Mice heterozygous for apelin were intercrossed and their offspring were obtained. The frequency of mutant homozygotes obtained in heterozygote intercrosses was close to the expected 25%, suggesting that apelin-deficient mice are not embryonically lethal. Although a small population of apelin-mutant mice lacked eyes and lost a great deal of weight, for reasons that have not been determined as yet, generally, the mutant animals appeared healthy as adults. Crosses between homozygous apelin-mutant animals were also fertile, indicating that implantation and embryonic development can apparently occur normally even when apelin is absent from both the embryo and the mother.

As apelin deficiency in *Xenopus* leads to severe disorganized blood vessel formation (Cox *et al*, 2006; Inui *et al*, 2006) and might induce embryonic lethality, it is possible that other unknown molecules compensate and rescue apelin deficiency in mammals. Before a compensatory effect was investigated, we studied the ISV at E9.5 (Figure 7A–C and Supplementary Figure 10), because we found that APJ expression was clearly observed in vessels sprouted from the DA into the somite (Figure 6). The results showed that body size and number of somites were equivalent between WT and apelin-mutant embryos at E9.5, but that the caliber of ISVs was narrower in apelin-deficient embryos compared with WT embryos. The expression of APJ was observed in all ECs of ISV sprouted from the DA, ranging from the base region of the sprout to the migrating end at E8.5; the expression had disappeared in the base region near the DA at E9.5 (Figure 6). This expression pattern in the phenotype of apelin-deficient embryos suggests that APJ expression is regulated by VEGF or other unknown molecules in ECs at the migrating end, in order to regulate the caliber size of blood vessels.

General Angl administration has been reported to induce enhancement of blood vessel formation in the trachea of adult mice (Cho *et al*, 2005). This indicates that tracheal blood vessels are active in angiogenesis in adulthood and it is possible that apelin deficiency affects blood vessel formation in this region. As expected, the blood vessels observed in the trachea of apelin-deficient mice were narrower than those in WT mice and, in addition, the capillary density was lower (Figure 8). Moreover, the blood vessels observed in the dermis (Figure 9 and Supplementary Figure 11) and heart (data not shown) of apelin-deficient mice were narrower than those in WT mice.

Through the use of the *in situ* hybridization method of APJ expression, it has been reported that APJ is not expressed on larger vessels such as DA, except for the posterior cardinal vein during early embryogenesis at around E9.5 (Devic *et al*, 1999). This result is consistent with our immunohistochemical analysis. The caliber sizes of the aorta and vena cava, and their major branches such as brachiocephalic, subclavian and common iliac arteries and veins, were not affected by the lack of apelin (data not shown). Therefore, this suggests that apelin may not be involved in the regulation of caliber size of larger vessels. Moreover, although apelin deficiency in *Xenopus* led to severely disorganized blood vessels in the vitelline (Cox *et al*, 2006; Inui *et al*, 2006), it did not affect the remodelling of blood vessels in the yolk sac (Supplementary Figure 12).

In order to analyse precisely the function of the exogenous apelin in the *in vitro* culture system, it was necessary to exclude from the analysis any confounding effects of the contaminating apelin from the culture serum, as well as the endogenous apelin produced from cultured cells. In order to achieve this, we tried to culture the aorta ring from apelin-deficient mice under quite low serum-containing conditions (Figure 7D and E). Although VEGF induced sprouting of ECs from the aorta, apelin on its own did not. However, the caliber size of VEGF-induced sprouts was enlarged upon the addition of apelin. Most of the sprouts induced by VEGF plus apelin contained large luminal cavities (data not shown). Therefore, we confirmed that apelin regulates caliber change in angiogenesis and this effect is induced in the

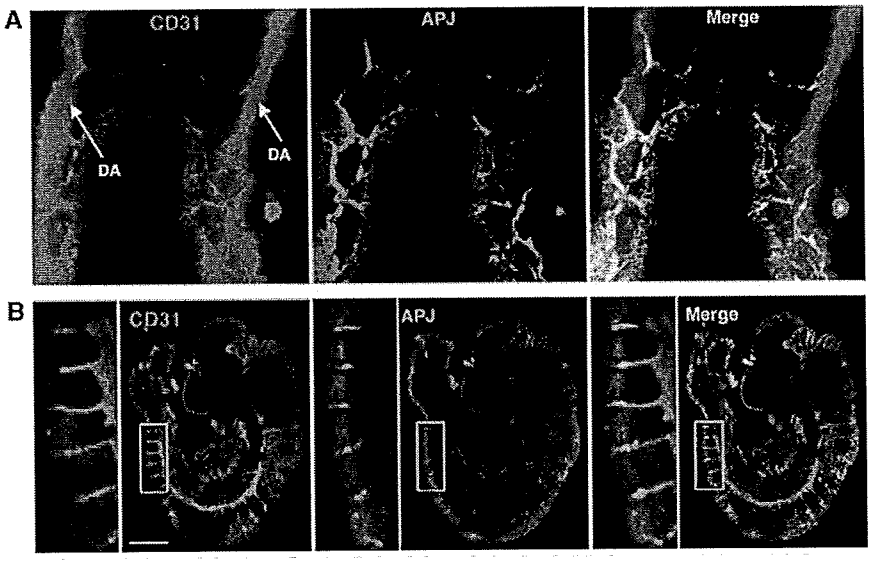

Figure 6 Expression of APJ in embryo. (**A**) Whole-mount staining of E8.5 mouse embryo with anti-CD31 (red) and anti-APJ (green) antibodies. (**B**) Staining of E9.5 mouse embryo section with anti-CD31 (red) and anti-APJ (green) Abs. The left panel shows high-power view of the area indicated by the box. Note that the DA stained by anti-CD31 Ab did not express APJ and APJ expressed on ECs sprouting from DA. Scale bar indicates 500 μm.

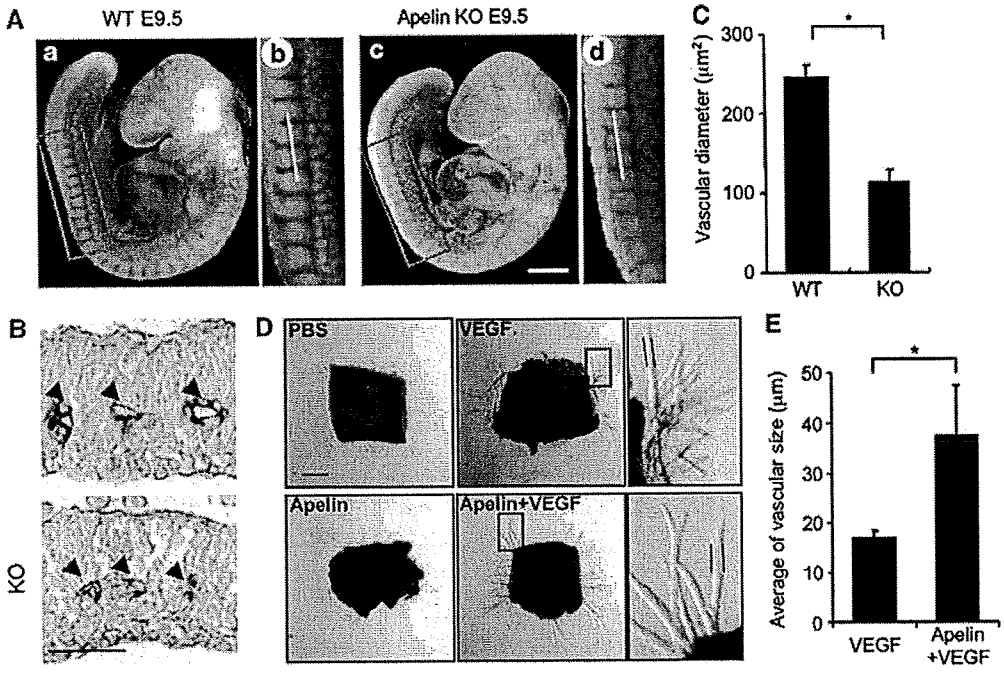

Figure 7 Defect of the enlargement in blood vessel caliber in apelin-deficient mice. (**A**) Whole-mount immunohistostaining of WT (a, b) and apelin-deficient (c, d) embryos at E9.5 with anti-CD31 Ab. (b) and (d) are higher magnifications of the areas indicated by the box in (a) and (c), respectively. Scale bar indicates 300 μm. (**B**) Sections containing ISVs (arrowheads) from WT and apelin-deficient (KO) embryos at E9.5 were stained with anti-CD31 antibody. The level of the sectioning position is indicated by a white bar in (b) and (d). Scale bar indicates 30 μm. (**C**) Quantitative evaluation of the vascular diameter of intersomitic blood vessels from apelin-deficient (KO) versus WT mice. $^*P<0.001$ (30 vessels from 5 embryos were examined). Details of the measurement of vascular diameter are shown in Supplementary Figure 7. (**D**) Representative pictures of microvessels sprouted from aortic ring using apelin-deficient mice. Aortic ring was cultured in the presence or absence of VEGF (10 ng/ml) or apelin (100 ng/ml). PBS was used as a negative control. Pictures in the right panel show a high-power view of the area indicated by the box, respectively. Scale bar indicates 300 μm. (**E**) Quantitative evaluation of the vascular size of sprouted microvessels from the aortic ring cultured as described in (D). Vascular size was measured as the length between two parallel lines as indicated in (D). $^*P<0.003$ ($n=30$).

absence of blood flow. It is known that blood flux regulates vessel size (Koller and Huang, 1999). Therefore, it is possible that shear stress may induce apelin expression in ECs. However, the results were contrary to our expectation. *In vitro* shear stress on HUVECs attenuated apelin mRNA expression in HUVECs (Supplementary Figure 13).

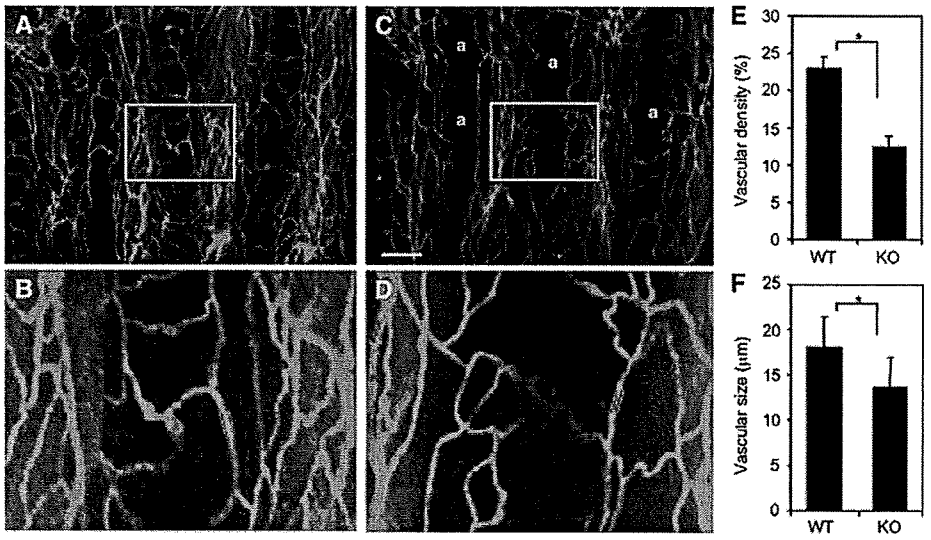

Figure 8 Lectin staining of tracheal blood vessels. (A–D) Comparison of tracheal blood vessels in 8-week-old WT (**A, B**) and apelin-deficient (**C, D**) mice stained by intravenous injection of fluorescein-labelled lectin. a in (C) means avascular area. (B) and (D) show a high-power view of the area indicated by the box in (A) and (C), respectively. Scale bar in (C) indicates 200 μm (A, C) and 60 μm (B, D). (**E**) Quantitative evaluation of vascular density from apelin-deficient (KO) versus WT mice. $^*P<0.001$. Vascular density from 10 random fields was counted. (**F**) Quantitative evaluation of vascular size of blood vessels in the trachea from apelin-deficient (KO) versus WT mice. Vascular size was measured as the length between two parallel red lines as indicated in (B) and (D). $^*P<0.001$ (100 vessels from 3 mice were examined).

Role of apelin in Ang1-induced enlargement of capillary size

We isolated apelin from ECs under the activation of Tie2 by Angl. Next, using apelin-deficient mice, we observed whether Angl-induced enlargement of blood vessels is suppressed in the absence of apelin. In this experiment, we mated apelin-deficient mice with Angl Tg mice and observed the caliber size of the capillaries in the dermis (Figure 9).

In apelin-deficient mice, the caliber size of the capillary in the dermis was narrower compared with that in WT mice (Figure 9A and B and Supplementary Figure 11). We confirmed that CD31-positive cells are from blood vessels but not from lymphatic vessels, by double staining with LYVE1, a specific marker for lymphatic ECs (Supplementary Figure 11). As previously reported (Suri *et al*, 1998), Angl Tg mice showed enlarged capillary formation in the dermis, but this effect of Angl was abolished by the lack of apelin (Figure 9A and B). However, apelin deficiency did not completely suppress Angl-induced enlargement of blood vessels, suggesting that other molecules upregulated by Tie2 activation might be involved in the caliber size determination of capillaries *in vivo*. On the other hand, the generation of extremely enlarged blood vessels, with a caliber size of more than $10^4\,\mu m^2$, observed in Angl Tg mice, was completely suppressed in the absence of apelin (Figure 9A and C). Therefore, we concluded that one of the molecules affected by Angl for enlargement of the capillary was apelin in ECs.

Apelin induces an enlarged endothelial sheet in P-Sp culture system

In vivo analysis suggested that apelin regulates the caliber change of blood vessels. Next, we observed blood vessel formation by using *in vitro* (P-Sp) organ culture system, which has previously been shown to mimic *in vivo* vasculogenesis and angiogenesis (Takakura *et al*, 1998, 2000). P-Sp explants from mice at E9.5 contain early developed DA. In the P-Sp culture system, ECs show two different morphologies. One is a sheet-like structure (vascular bed) that develops in the early stages of the culture. The other is a network-like structure, constructed from the ECs sprouting from the vascular bed. Previously, we identified that the sheet-like formation mimics vasculogenesis and the network formation mimics angiogenesis, which is a process of capillary sprouting from pre-existing vessels (Takakura *et al*, 2000). Therefore, as apelin-mutant embryos showed narrow ISVs, which were sprouted from the DA, this suggests that the P-Sp culture system can reproduce the *in vivo* effects of apelin.

In the P-Sp culture system, OP9 stromal cells were used as feeder cells for P-Sp explants. We induced apelin expression on OP9 cells (Figure 3B) and observed the effect. Compared to the control culture (Figure 10Aab), network-forming ECs became thick and the vascular density of the network area was high (Figure 10Acd), although the amount of branching was the same. By contrast, the suppression of apelin/APJ function, by blocking antibody against apelin, induced thin network formation by ECs (Figure 10Aef). When the network-forming area of ECs was evaluated, it was higher in apelin-expressing OP9 cells (OP9/apelin) than in control OP9 cells (OP9/vector); this effect by apelin was completely blocked by anti-apelin mAb (Figure 10Ag).

In the P-Sp culture system, we found that APJ is expressed in the network-forming ECs sprouted from the vascular bed as observed in the ISVs, but not in the ECs forming the sheet (Figure 10B). *In vitro* analysis indicated that the apelin/APJ system might affect cell-to-cell aggregation or assembly, and therefore we stained network-forming ECs by anti-VE-cadherin antibody. As observed in Figure 10C, apelin enhanced the assembly of ECs. Interestingly, in the control P-Sp culture, the network-forming endothelial layer, composed of one or two ECs, migrated in a peripheral direction along with the ECs at the tip (Figure 10Cab). On the other hand, when apelin was overexpressed on OP9 cells, many aggregated

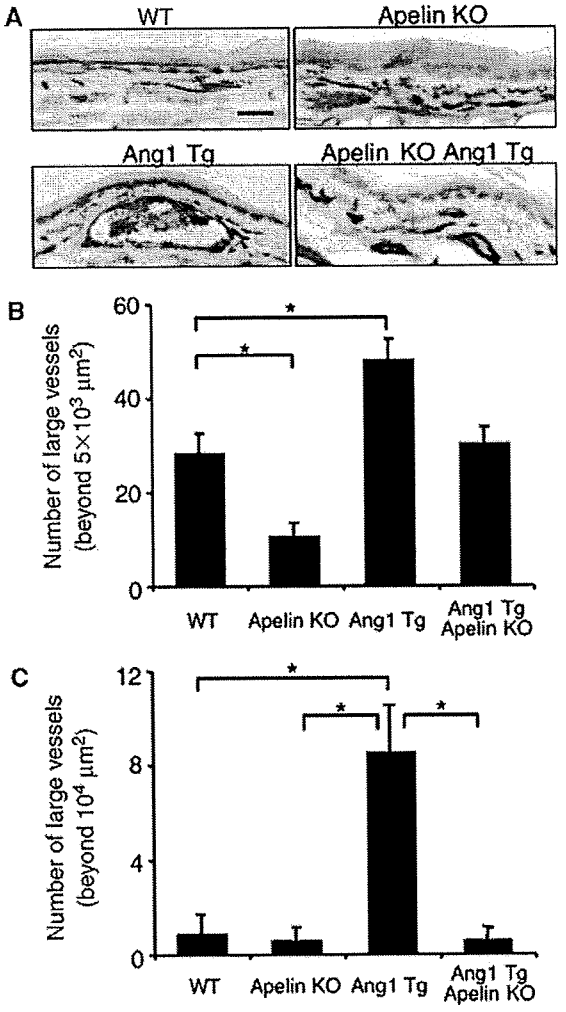

Figure 9 Apelin/APJ system is involved in Angl-induced vascular enlargement. (**A**) Sections of ear skin stained with anti-CD31 mAb. Ear skin was prepared from 8-week-old WT, apelin-deficient (apelin KO), Angl Tg mice, or apelin-deficient mice mated with Angl Tg mice (apelin KO/Angl Tg). Scale bar indicates 30 μm. (**B**, **C**) Quantitative evaluation of the number of enlarged blood vessels composed of a luminal cavity of more than 5000 μm^2 (B) or more than 10^4 μm^2 (C) in the skin from mice as described in (A). Thirty random fields were observed from sections of three independent mice as described in (A). $^*P<0.01$.

ECs migrated along with the ECs at the tip (Figure 10Ccd), and this effect was completely suppressed by anti-apelin mAb (Figure 10Cef). These results indicated that apelin induces an enlarged endothelial sheet when angiogenesis is taking place.

Discussion

The knowledge of how vascular cells commit from their progenitor cells and generate a closed cardiovascular circulatory system has accumulated in recent years, mostly by the isolation and functional analysis of molecules associated with blood vessel formation. However, little is known regarding the molecular events that regulate EC morphogenesis, especially the caliber size determination of blood vessels. Data documented here, from both *in vitro* and *in vivo* analysis, showed that apelin regulates the enlargement of newly developed blood vessels during angiogenesis.

In angiogenesis, how blood vessels 'decide' their appropriate size is very important to the organization of the adjustment of tissue and organ demand for oxygen and nutrients. Our analysis clearly showed that APJ expression was induced by VEGF, which, in turn, is well known to be induced by tissue hypoxia (Liu *et al*, 1995). This indicates that, under tissue hypoxia, blood vessels have an opportunity to enlarge their size and the reduction of APJ expression finalizes the enlargement of blood vessel caliber under tissue normoxia. Indeed, in the retina, APJ was observed temporally in the radial vessels and the associated capillaries of retina from day 3 to day 12 after birth, but APJ expression on ECs was attenuated in the later stage (Saint-Geniez *et al*, 2002). As reported in the retina, we also found that APJ expression was observed in ECs sprouted from the DA and ECs on blood vessels in the neonatal dermis of mice (data not shown), but that it gradually disappeared with maturity. These expression patterns strongly suggested that APJ plays a spatio-temporal role in the maturation of blood vessels by transient expression on ECs of blood vessels where angiogenesis is taking place. Therefore, we concluded that one of the molecules associated with the regulation of blood vessel diameter was apelin in the ECs.

Based on our results presented here, it appears that VEGF, Angl and apelin regulate caliber size in a concerted fashion, as follows. Upon stimulation by VEGF, ECs sprouted from pre-existing vessels may express APJ. Subsequently, Angl stimulates these sprouted ECs to induce apelin expression. In the presence of both VEGF and apelin, the ECs start to proliferate, adhere and form contacts with each other through junctional proteins, and construct enlarged blood vessels. Apelin has been reported to induce angiogenesis in the Matrigel plug assay (Kasai *et al*, 2004) and also chemotaxis (Cox *et al*, 2006). In our experiments using the Matrigel plug assay, we found that apelin induced migration, rather than proliferation, of ECs (Supplementary Figure 14). Moreover, we confirmed that like VEGF, apelin modified the cytoskeleton structure (Supplementary Figure 15). Therefore, apelin may induce mobilization of ECs in the process of EC-to-EC assembly.

As we found, apelin deficiency suppressed the enlargement of ISVs during early embryogenesis. Furthermore, it has been reported elsewhere that Angl and VEGF are expressed in intersomitic or somitic tissues (Davis *et al*, 1996; Lawson *et al*, 2002) and that apelin is coexpressed with APJ-positive ECs in ISVs. Indeed both Tie2 and Angl mutant embryos showed impaired ISV formation (Dumont *et al*, 1994; Sato *et al*, 1995). Therefore, it appears that these three components may be involved in the regulation of caliber size change of the ISVs.

Transgenic overexpression of Angl in the keratinocyte induced enlarged blood vessels in the dermis (Suri *et al*, 1998) and administration of a potent Angl variant was also reported to induce enlargement of blood vessels (Cho *et al*, 2005; Thurston *et al*, 2005). Therefore, Angl expression may be a key determinant of caliber size during angiogenesis. Angl is usually produced from MCs in cells composing blood vessels (Davis *et al*, 1996), However, we previously reported that hematopoietic stem cells (HSCs) producing Angl migrate into avascular areas before the ECs start to migrate, and that this Angl from HSCs induces angiogenesis by promoting the chemotaxis of ECs (Takakura *et al*, 2000). Moreover, recently,